Molecular Plant
Research article

CellPress
Partner Journal

Spatiotemporal oxygen dynamics in young leaves reveal cyclic hypoxia in plants

Paolo M. Triozzi[1,2], Luca Brunello[1], Giacomo Novi[1], Gianmarco Ferri[3], Francesco Cardarelli[4], Elena Loreti[5], Mariano Perales[2,6] and Pierdomenico Perata[1,*]

[1]PlantLab, Center of Plant Sciences, Sant'Anna School of Advanced Studies, 56010 Pisa, Italy

[2]Centro de Biotecnología y Genómica de Plantas, Universidad Politécnica de Madrid (UPM)–Instituto Nacional de Investigación y Tecnología Agraria y Alimentaria (INIA-CSIC), Campus de Montegancedo UPM, Pozuelo de Alarcón, 28223 Madrid, Spain

[3]Fondazione Pisana per la Scienza, 56017 Pisa, Italy

[4]Laboratorio NEST, Scuola Normale Superiore, Istituto Nanoscienze-CNR, Piazza S. Silvestro, 12, 56127 Pisa, Italy

[5]Institute of Agricultural Biology and Biotechnology, National Research Council, 56124 Pisa, Italy

[6]Departamento de Biotecnología-Biología Vegetal, Escuela Técnica Superior de Ingeniería Agronómica, Alimentaria y de Biosistemas, Universidad Politécnica de Madrid (UPM), 28040 Madrid, Spain

***Correspondence: Pierdomenico Perata (p.perata@santannapisa.it)**

https://doi.org/10.1016/j.molp.2024.01.006

ABSTRACT

Oxygen is essential for plant growth and development. Hypoxia occurs in plants due to limited oxygen availability following adverse environmental conditions as well in hypoxic niches in otherwise normoxic environments. However, the existence and functional integration of spatiotemporal oxygen dynamics with plant development remains unknown. In animal systems dynamic fluctuations in oxygen availability are known as cyclic hypoxia. In this study, we demonstrate that cyclic fluctuations in internal oxygen levels occur in young emerging leaves of *Arabidopsis* plants. Cyclic hypoxia in plants is based on a mechanism requiring the ETHYLENE RESPONSE FACTORS type VII (ERFVII) that are central components of the oxygen-sensing machinery in plants. The ERFVII-dependent mechanism allows precise adjustment of leaf growth in response to carbon status and oxygen availability within plant cells. This study thus establishes a functional connection between internal spatiotemporal oxygen dynamics and developmental processes of plants.

Key words: *Arabidopsis*, hypoxia, cyclic hypoxia, leaf development, oxygen-sensing mechanism, ERFVII

Triozzi P.M., Brunello L., Novi G., Ferri G., Cardarelli F., Loreti E., Perales M., and Perata P. (2024). Spatiotemporal oxygen dynamics in young leaves reveal cyclic hypoxia in plants. Mol. Plant. **17**, 377–394.

INTRODUCTION

As aerobic organisms, higher plants need oxygen to grow and survive (Bailey-Serres and Voesenek, 2008). Oxygen is the final acceptor in the electron transport chain and is essential for ATP production in the mitochondria of eukaryotic cells (Millar et al., 2011). Insufficient oxygen compromises many cellular functions including mitochondrial respiration, ATP production, and energy supply, eventually leading to death (Perata and Alpi, 1993; Bailey-Serres and Voesenek, 2008). Plants frequently encounter low oxygen conditions due to a sudden drop in oxygen concentration in the environment, a high rate of cellular respiration in proliferative tissues, or limited diffusion caused by anatomical barriers (Loreti et al., 2016; Weits et al., 2021). When plant cells experience a decline in oxygen concentrations, they enter a hypoxic status, triggering adaptive responses to cope with the energy crisis induced by low oxygen (Loreti et al., 2005; Lasanthi-Kudahettige et al., 2007; Bailey-Serres and Voesenek, 2008; Mustroph et al., 2009, 2010; Narsai et al., 2011; Van Dongen and Licausi, 2015). One of the primary cellular adaptative mechanisms involves activating the hypoxic metabolism, which allows limited energy production and re-oxidation of reduced compounds produced during glycolysis via the fermentative pathways (Loreti et al., 2016; Cho et al., 2021).

In *Arabidopsis*, this switch from aerobic to hypoxic metabolism is controlled by a class of transcription factors, known as the ETHYLENE RESPONSE FACTORS that belong to group VII (ERFVIIs) (Licausi et al., 2011b; Gibbs et al., 2011). In the presence of oxygen, ERFVIIs are oxidized following methionine removal by METHIONINE AMINO-PEPTIDASE (MAPs) (Holdsworth et al., 2020) at the cysteine at the N-terminus by the PLANT CYSTEINE OXIDASES (PCOs) (Bailey-Serres and

Published by the Molecular Plant Shanghai Editorial Office in association with Cell Press, an imprint of Elsevier Inc., on behalf of CSPB and CEMPS, CAS.

Voesenek, 2008; Van Dongen and Licausi, 2015). Oxidized cysteine is arginylated by ARGINYL TRANSFERASEs (ATEs) (White et al., 2017), which target the ERFVIIs for proteasomal degradation via the E3 ligase PROTEOLYSIS6 (PRT6) N-degron pathway (Van Dongen and Licausi, 2015; Holdsworth et al., 2020; Loreti and Perata, 2020). However, under hypoxic conditions, ERFVII oxidation cannot occur due to the absence of molecular oxygen, which hampers PCO activity (Taylor-Kearney and Flashman, 2022). ERFVIIs do not undergo proteasomal degradation, instead they become stable and they translocate to the nucleus to activate the expression of hypoxia-responsive genes (HRGs), which include those involved in fermentation (Mustroph et al., 2009). The activation of HRGs is crucial for the survival of the plant under extreme environmental conditions, such as flooding. Such conditions can lead to soil waterlogging, when only the roots are completely under the water level, or submergence where the entire plant is under water. Both conditions negatively affect plant growth and development (Van Dongen and Licausi, 2015; Loreti et al., 2016).

Given that starch is the main source of sugars for energy production when photosynthesis is limited or absent, it is essential for plant survival as well as for the induction of *ALCOHOL DEHYDROGENASE* (*ADH*) and other anaerobic genes under submergence (Loreti et al., 2018). Moreover, the energy-sensing TARGET OF RAPAMYCIN (TOR) pathway is deployed to ensure that the hypoxic responses match the current energy status of the plant cell (Kunkowska et al., 2023). Therefore, the transcriptional activation of HRGs is integrated with sugar availability to generate an appropriate adaptive response according to the energetic status of the plant.

Plant responses to low oxygen have been extensively studied in the context of abiotic stress events, when sudden lack of oxygen may occur as a consequence of soil flooding, leading to an acute hypoxic status in the plant (Bailey-Serres and Voesenek, 2008; Loreti et al., 2016; Loreti and Perata, 2020). However, hypoxic niches where oxygen levels are locally and constitutively maintained low in plants have recently been discovered. This kind of hypoxia is known as chronic hypoxia (Weits et al., 2021) and has been found in the meristem regions, including shoot and root apical meristems and lateral root primordia, where it does not subject the cells to stress but is actually essential for plant development (Gibbs et al., 2018; Shukla et al., 2019; Weits et al., 2019; Labandera et al., 2021). In these hypoxic niches, the PROTEOLYSIS6 (PRT6) N-degron substrates LITTLE ZIPPER2 (ZPR2) and VERNALIZATION2 (VRN2) act as regulators of plant development (Weits et al., 2019; Labandera et al., 2021). Chronic hypoxia thus represents an essential developmental signaling cue and differs from the acute hypoxia, which is typically generated as a consequence of unpredictable flooding and is perceived as stress by the plant (Bailey-Serres and Voesenek, 2008; Loreti et al., 2016; Weits et al., 2021).

Although acute and chronic hypoxia have distinct origins and effects on plant growth and survival, both conditions define a quasi-steady state of low oxygen levels over time. In the context of cancer research, dynamic oxygen changes have been studied extensively. Within a tumor, oxygen levels fluctuate due to changes in red blood cell flux, vascular remodeling, and thermoregulation (Michiels et al., 2016; Bader et al., 2020). These fluctuations in oxygen levels, also known as transient or cyclic hypoxia, have significant biological relevance for the tumor growth (Bader et al., 2020).

The perception of oxygen fluctuations in human cells relies on the oxygen-dependent degradation of the hypoxia inducible factor 1α (HIF-1α) transcription factor (Wang et al., 1995), through a pathway that shares similarities with the PRT6 N-degron pathway in plants (Holdsworth and Gibbs, 2020; Licausi et al., 2020). During normoxia, HIF-1α is degraded via the ubiquitin–proteasome pathway, whereas during hypoxia, it is stabilized and protected from proteolysis, allowing its translocation into the nucleus, where it forms a complex with HIF-1β and induces the transcription of hypoxic genes. Similarly, in higher plants, internal oxygen dynamics could occur due to high cellular respiration rate, reduction or inhibition of photosynthetic activity, limited diffusion of oxygen due to stomatal movement but also due to plant organ or tissue type. A meta-analysis of plant tissue O_2 measurements from 112 different plant species recently highlighted how hypoxic conditions develop particularly in thick tissues and some roots, while hyperoxic conditions are observed in submerged, photosynthesizing tissues (Herzog et al., 2023). In addition, the main factors driving plant tissue O_2 dynamics are submergence, light, and tissue type (Herzog et al., 2023). Interestingly, although internal oxygen dynamics have been measured using different methods in plants, the existence of cyclic hypoxia and its functional link with developmental processes has not been reported in plants so far.

Here, we provide evidence for the existence of cyclic hypoxia in plants, characterized by a temporary decrease in oxygen levels in young emerging leaves at night. This nocturnal hypoxia triggers the hypoxic response via the ERFVII-dependent pathway, thereby creating a metabolic switch from oxic to hypoxic pathway to generate competition between aerobic and hypoxic metabolism. This then enables the plant to sustain leaf growth according to carbon sources and oxygen availability.

RESULTS

Diurnal patterns of HRGs reveal cyclic hypoxia in plants

We hypothesized that, if daily oxygen dynamics occur within the plant, HRGs would exhibit diurnal patterns of gene expression. We analyzed diurnal genome-wide expression data from the Diurnal repository (Mockler et al., 2007). We found that 42 out of 49 core HRGs (Mustroph et al., 2009) displayed robust diurnal patterns of gene expression under light/dark cycles (supplemental Figure 1 and supplemental Table 1). A total of 27 genes (~65%) belonging to clusters 1, 6, 7, and 8 were activated overnight, while 15 genes (~35%) from clusters 2, 3, 4, and 5 showed a peak in the daytime (supplemental Figure 1). Thus, cyclic hypoxia might occur in plants and be responsible of diurnal patterns of HRGs.

To investigate the diurnal regulation of HRGs, we conducted a time-course experiment using *Arabidopsis* seedlings grown under long day (LD) conditions. First, we analyzed the gene expression of *CIRCADIAN CLOCK-ASSOCIATED 1* (*CCA1*) gene. *CCA1* showed its typical circadian pattern (supplemental

Figure 2), as previously observed (Mizoguchi et al., 2002). We then examined the gene expression of key HRGs including *ADH*, *PCO1*, *PHYTOGLOBIN1* (*PGB1*), *LOB DOMAIN-CONTAINING PROTEIN 41* (*LBD41*), *WOUND-INDUCED POLYPEPTIDE 4* (*WIP4*), *HYPOXIA UNKNOWN PROTEIN 7* (*HUP7*), *HYPOXIA RESPONSE ATTENUATOR 1* (*HRA1*), and *PCO2*. These genes exhibited nighttime induction, with maximum activation at ZT20 (Figure 1A).

Furthermore, to assess the contribution of transcription to the diurnal patterns of HRGs (hereafter "cyclic HRGs" [cHRGs]), we analyzed the activity of two transcriptional reporters: *pPGB1:LUC* and *pPCO1:LUC*. These reporters consist of the full promoters of *PGB1* (Licausi et al., 2011a) and *PCO1* (Weits et al., 2014), respectively, and they guide the expression of firefly luciferase. *In vivo* monitoring of these reporters revealed that both promoters were induced during the night (Figure 1B and 1C and supplemental Figure 3A and 3B). Interestingly, the transcriptional activation was sharper starting from day 2 and reached the maximum on days 3 and 4 (Figure 1B and 1C and supplemental Figure 3A and 3B), suggesting a potential involvement of plant development on their transcriptional activation. Collectively, these results support the existence of cyclic hypoxia in plants.

Cyclic hypoxia is an ERFVII-dependent response

Many of the diurnal rhythms in plants are controlled by a central oscillator known as the circadian clock (Webb, 2003). We thus investigated whether cyclic hypoxia could be controlled by the circadian clock or might result from a drop in internal oxygen during the night. Under continuous light (CL) or darkness conditions, the clock continues to oscillate with its endogenous period (Harmer et al., 2000; Dalchau et al., 2011). Hyperoxia treatment of cancer cells has been shown to inhibit endogenous hypoxia response (Kim et al., 2020). To unravel the regulation of cyclic hypoxia, gene expression of cHRGs was evaluated under CL and nocturnal hyperoxia conditions, collecting samples in the morning (ZT4) and at night (ZT20; Figure 2A), when cHRGs exhibited the minimum and maximum of expression, respectively (Figure 1A). The data showed that CL totally abolished the activation of cHRGs (Figure 2B), indicating that the oscillatory behavior of cHRGs is not controlled by the clock. Similarly, nocturnal hyperoxia treatment significantly reduced the activation of cHRGs, suggesting that cyclic hypoxia can be generated because of a drop in endogenous oxygen levels during the night (Figure 2B).

According to the RT–qPCR results, the switch from LD to CL abolished *PGB1* and *PCO1* promoter activation in the subjective night (Figure 2C and 2D). As observed for the mRNA levels, nocturnal hyperoxia significantly dampened *pPGB1:LUC* and *pPCO1:LUC* activity compared with normoxic night (Figure 2E and 2F), pointing out that cyclic hypoxia is controlled at the transcriptional level.

Since low oxygen levels stabilize ERFVII proteins, which in turn trigger the transcriptional activation of HRGs, we analyzed whether ERFVII protein steady-state level was influenced at a different time of the day using a previously characterized *35S:RAP2.3*^{3xHA} Arabidopsis line (Gibbs et al., 2014). RAP2.3^{3xHA} level was higher during the nighttime compared with the daytime (Figure 3A). The stabilization of RAP2.3^{3xHA} in the night was antagonized after 4 h of hyperoxia in the night (Figure 3B). Gene expression of cHRGs was analyzed in the pentuple *erfVII* mutant (which lacks the five members of ERFVII family; Abbas et al., 2015) and Col-0 in a 24-h time-course experiment to evaluate the contribution of ERFVIIs to cyclic hypoxia. Gene expression of *ADH*, *HUP7*, and *PCO2* was much lower or totally abolished in the *erfVII* mutant (Figure 3), whereas the other cHRGs were still slightly expressed during the night, suggesting that, besides ERFVIIs, other factors might participate in the regulation of cHRGs. We also tested whether ERFVIIs could control the circadian clock gene expression. The clock gene *CCA1* showed a similar circadian pattern in *erfVII* and Col-0; however, it was significantly downregulated and upregulated at ZT8 and ZT20, respectively, in *erfVII* mutant compared with Col-0 (supplemental Figure 4).

Analysis of cHRGs in *prt6* and *ate1ate2* double mutant, in which PRT6 N-degron pathway substrates including ERFVIIs are constitutively stable (Licausi et al., 2011b; Gibbs et al., 2011), showed that cHRGs were induced at ZT20 compared with ZT4 (supplemental Figure 5A and 5B). This result indicates that, even in the presence of constitutive stable PRT6 N-degron pathway substrates, the night induced higher cHRGs expression in *prt6* and *ate1ate2* double mutant.

The PCO branch of the PRT6 N-degron pathway requires not only oxygen but also nitric oxide (NO) for destabilization of ERFVIIs (Gibbs et al., 2014). In plants, NO is mainly produced via nitrate reductase, whose activity is well known to be diurnal, very reduced at night, and showing a maximum of activity in the morning (Pilgrim et al., 1993). Endogenous NO is mainly localized in guard cells in young emerging leaves both at ZT4 and ZT20 (supplemental Figure 6A), in line with the NO-mediated ERFVII degradation in controlling stomatal aperture reported previously (Gibbs et al., 2014). The expression of some cHRGs in the NO-deficient triple mutant (*nia1nia2noa1-2*) and NO overproducer mutant (*cue1-6*) was altered at ZT20 coherently with a role of NO in de-stabilizing the ERFVIIs (supplemental Figure 6B). However, the expression of several cHRGs at ZT20 was repressed in both *nia1nia2noa1-2* and *cue1-6*. Since both mutants showed smaller plant size and less tissue density, possibly leading to less severe hypoxia and thus influencing cHRGs diurnal patterns, we assessed cyclic hypoxia responses after altering NO endogenous levels in wild-type seedlings either by applying the NO donor SNAP (S-nitroso-N-acetyl-DL-penicillamine) at night or the NO scavenger cPTIO (carboxy-PTIO potassium salt) at the beginning of the day. SNAP was able to significantly downregulate *pPGB1:LUC* activity but not *pPCO1:LUC* (supplemental Figure 6C), whereas cPTIO at the beginning of the day led to increased *pPCO1:LUC* activity after 4 h without affecting *pPGB1:LUC* (supplemental Figure 6D).

We also analyzed the diurnal gene expression of N-degron pathway enzymes as they might contribute to the observed changes in cHRGs through the regulation of ERFVII stability. We found that *MAP2A*, *PCO3*, *PCO5*, *ATE1*, and *ATE2* showed increased gene expression at the end of the nighttime (supplemental Figure 7).

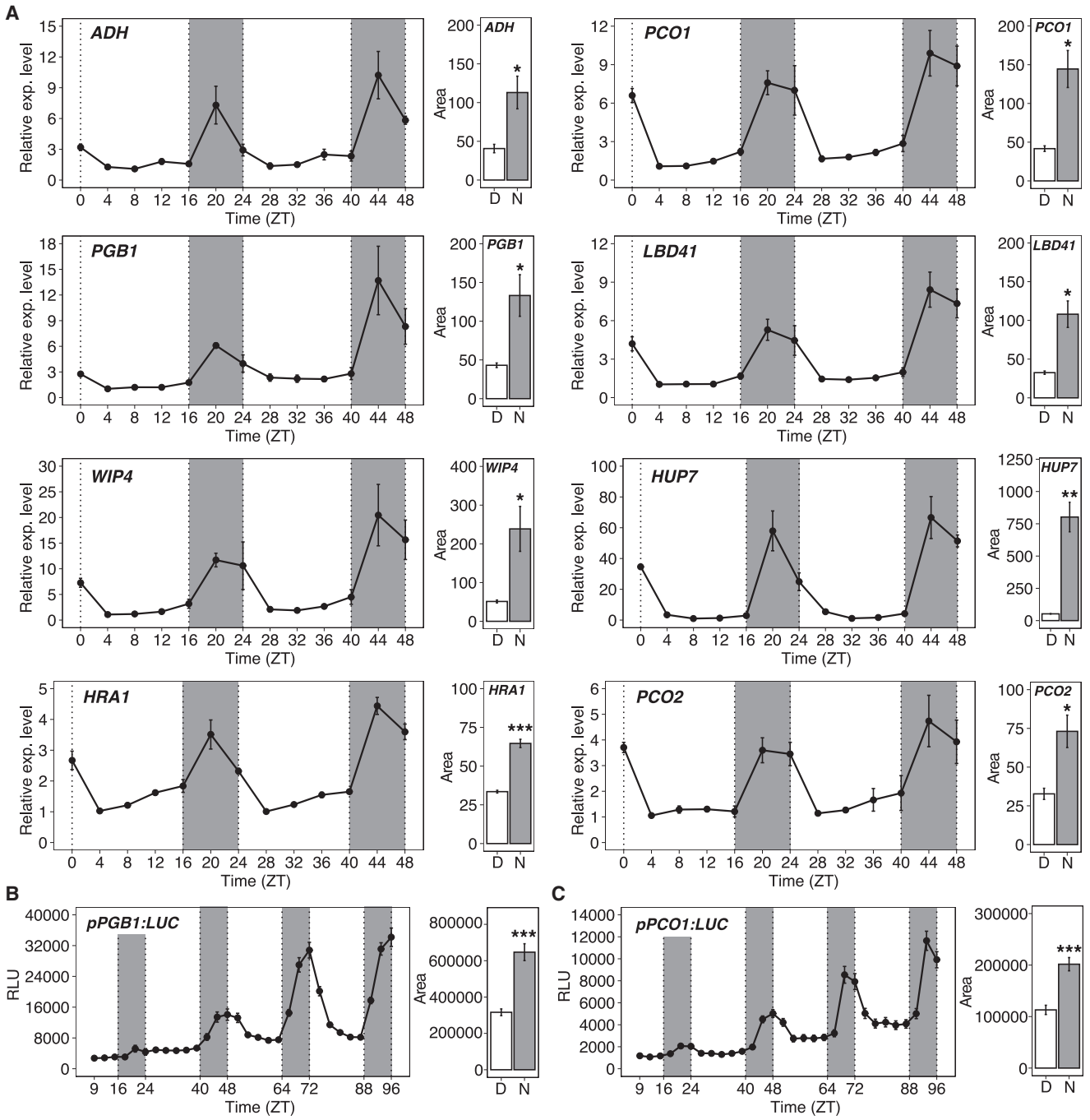

Figure 1. Hypoxia-responsive gene expression is activated at night.

(A) Gene expression analysis of hypoxia-responsive genes (*ADH*, *PCO1*, *PGB1*, *LBD41*, *WIP4*, *HUP7*, *HRA1*, and *PCO2*) in a time-course experiment using 6-day-old *Arabidopsis* Col-0 seedlings. Samples were collected every 4 h for 2 days. The mRNA levels of genes were measured by RT–qPCR, and the data on the y-axis are expressed relative to ZT4 (ZT4 = 1). The x-axis represents zeitgeber time (ZT0, the time when the lights are switched on). The data represent the mean ± standard error (SE) of three biological replicates. Overall levels of gene expression in the daytime (D) and nighttime (N) estimated by calculation of area under the curve. Student's *t*-test was performed, and asterisks indicate statistically significant differences of gene expression levels between day and night (*$P < 0.05$, **$P < 0.01$, ***$P < 0.001$).

(B and C) Luciferase activity of *pPGB1:LUC* and *pPCO1:LUC* seedlings (5 days old) detected by luminescence assay during 4 days under LD conditions. The y-axis represents relative luminescence units (RLU), while the x-axis represents time expressed in ZT. The data represent the mean ± SE (*pPGB1:LUC*, $n = 31$; *pPCO1:LUC*, $n = 16$). Overall levels of transcription in the daytime (D) and nighttime (N) estimated by calculation of area under the curve. Student's *t*-test was performed, and asterisks indicate statistically significant differences of gene expression levels between day and night (***$P < 0.001$).

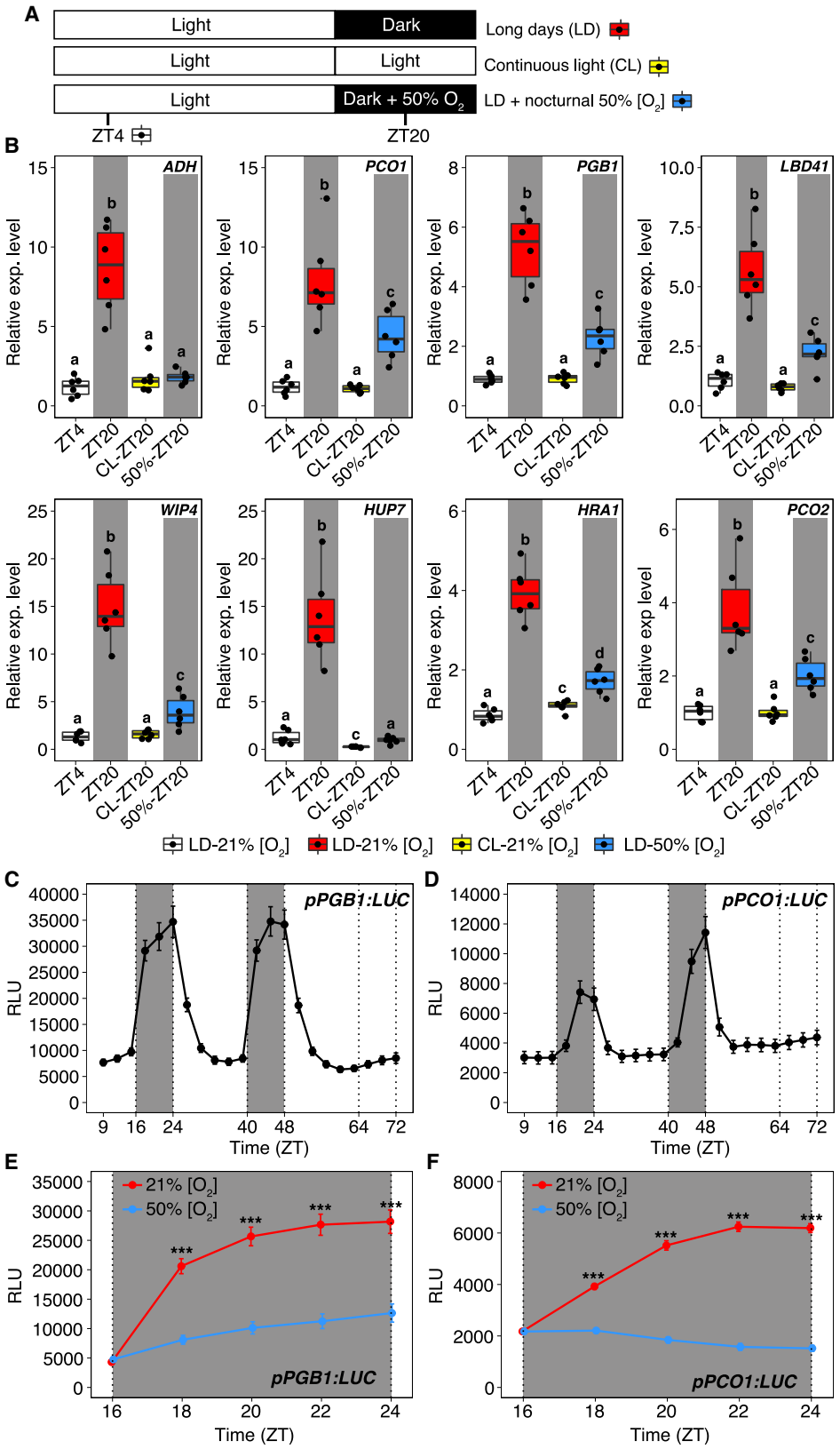

(legend on next page)

An interplay between cellular respiration and photosynthesis generates cyclic hypoxia in young emerging leaves

Diurnal patterns of cHRGs require the function of ERFVIIs (Figure 3). However, it is unclear whether cyclic hypoxia occurs in the whole plant or in a specific organ/tissue. To investigate the spatial occurrence of cyclic hypoxia, we analyzed the gene expression of cHRGs in the shoot and in the root compared with the whole seedling (supplemental Figure 8A). We observed a similar induction of cHRGs in the night in both the shoot and the whole seedling, while gene expression levels were significantly lower in the roots (supplemental Figure 8B), thus indicating that cyclic hypoxia mostly occurs in the aerial part of the plant.

We examined the β-glucuronidase (GUS) reporters *pADH:GUS*, *pPCO1:GUS*, and *pPGB1:GUS* during the night and at different developmental stages of the seedling: at 6, 8, and 10 days after germination (DAG). These analyses revealed predominant GUS staining in the shoot apical meristem (SAM) and in the young leaves of the shoot, which was consistent across the reporter lines analyzed (Figure 4A and supplemental Figure 9). Since the SAM is known to experience chronic hypoxia (Weits et al., 2019), it is unlikely that cyclic hypoxia occurs in the SAM. To better understand the spatio-temporal regulation of cyclic hypoxia, we analyzed cHRG expression of at 6, 8, and 10 DAG in the shoot in the morning (ZT4) and at night (ZT20).

If cyclic hypoxia is associated with leaf growth and development, we would expect different levels of cHRGs activation in relation to the different leaf developmental stages. We found that *ADH*, *PGB1*, *LBD41*, *WIP4*, *HRA1* showed a significant increase at night at DAG 8 and 10 compared with DAG 6 (Figure 4B and supplemental Figure 10). *PCO1* and *HUP7* also showed an increase at DAG 8 with respect to DAG 6, but this was not significantly different (supplemental Figure 10). Next, we monitored *pPGB1:LUC* and *pPCO1:LUC* activities using the NightSHADE instrument, allowing *in vivo* luciferase imaging for 2 days. We found that *pPGB1:LUC* and *pPCO1:LUC* were mainly expressed and induced in the young emerging leaves at night (supplemental Videos 1 and 2 and supplemental Figure 11). Overall, these results indicated that cyclic hypoxia occurred in young emerging leaves.

We therefore measured endogenous oxygen levels in young leaves at different times of the day and developmental stages (8 and 10 DAG) using a micro-Clark-type O_2 electrode. Our measurements revealed that the average of O_2 tension was approximately around 15% in the morning in young leaves at 8 DAG (Figure 4C), while it dropped down to around 10% at night (Figure 4C). However, older leaves at 10 DAG did not experience the same oxygen drop at night, with an average of 15.5% and 13.5% at ZT4 and ZT20, respectively (Figure 4C).

Actively growing leaves undergo simultaneous cell proliferation and expansion, and these two processes require a substantial amount of energy, which is provided by sustained cellular respiration (Gonzalez et al., 2012). We hypothesized that the mitochondrial activity in young leaves could lead to a temporary decrease in oxygen levels at night where the supply of O_2 only relies on gas diffusion, as there is no oxygen production through photosynthesis.

In fact, treatment with the cellular respiration inhibitor antimycin A (AA) at the beginning of the night led to a strong upregulation of *pPGB1:LUC* activity, whereas *pPCO1:LUC* was downregulated (Figure 4D). Similarly, AA treatment significantly reduced the activation of *ADH*, *PCO1*, *WIP4*, *HUP7*, *HRA1*, and *PCO2* genes at ZT20, whereas *LBD41* showed no differences compared with the control treatment (supplemental Figure 12A and 12B). Similar to *pPGB1:LUC* activity, *PGB1* gene expression was strongly activated in AA-treated plants (supplemental Figure 12B), likely as a result of the oxidative stress induced by this inhibitor (Giuntoli et al., 2017). Indeed, AA treatment induces the production of reactive oxygen species and arrest of cell proliferation due to impaired electron transport chain function in the mitochondria (Liu et al., 2023), which is supported by the activation and downregulation of oxidative stress and cell cycle markers, respectively (supplemental Figure 12C).

Carbon starvation inhibits mitochondrial activity by limiting respiration substrate availability (Contento et al., 2004). Thus, to prevent photosynthesis and the build-up of transitory starch required for nighttime respiration, we blocked the photosynthetic activity in the daytime with the DCMU (3-(3,4-dichlorophenyl)-1,1-dimethylurea) inhibitor (supplemental Figure 13A). This treatment resulted in an earlier carbon starvation condition, as evidenced by the strong upregulation of *DARK INDUCIBLE 6* (*DIN6*) gene, a carbon starvation marker, in the DCMU-treated plants at ZT20 (supplemental Figure 13B). At the same time, cHRG gene expression was significantly lower in plants that were treated with DCMU during the day compared with the control plants (supplemental Figure 13C). Besides the reduction of cellular respiration rate, limited availability of carbon resources leads to

Figure 2. Cyclic hypoxia is an oxygen-dependent response.

(A) The experimental setup showing different conditions and time points of sample collection.

(B) Gene expression analysis of hypoxia-responsive genes (*ADH*, *PCO1*, *PGB1*, *LBD41*, *WIP4*, *HUP7*, *HRA1*, and *PCO2*) at ZT4 and ZT20 under long days (LD), and at ZT20 under continuous light (CL) or LD + nocturnal hyperoxia treatment (LD + 50% [O_2]). The mRNA levels of genes were measured by RT–qPCR, and the data on the y-axis are expressed relative to ZT4 (ZT4 = 1). Statistical significance was calculated using Kruskal–Wallis test followed by post-hoc Wilcoxon test, and groups of significant difference ($P < 0.05$) are indicated with different letters ($n = 6$ biological replicates).

(C and D) Luciferase activity of *pPGB1:LUC* and *pPCO1:LUC* seedlings (8 days old) detected by luminescence assay for 2 days under LD and for an additional 24 h under CL. The data represent the mean ± SE ($n = 16$).

(E and F) Luciferase activity in *pPGB1:LUC* and *pPCO1:LUC* seedlings (8 days old) in air or hyperoxia in the night. Hyperoxia treatment started at the beginning of the night (ZT16). Statistical significance was calculated using the Kruskal–Wallis test at each time point. Asterisks represent statistically significant differences between the different conditions (***$P < 0.001$). The data represent the mean ± SE (*pPGB1:LUC*_21%, $n = 42$; *pPGB1:LUC*_50%, $n = 46$; *pPCO1:LUC*_21%, $n = 43$; *pPCO1:LUC*_50%, $n = 44$).

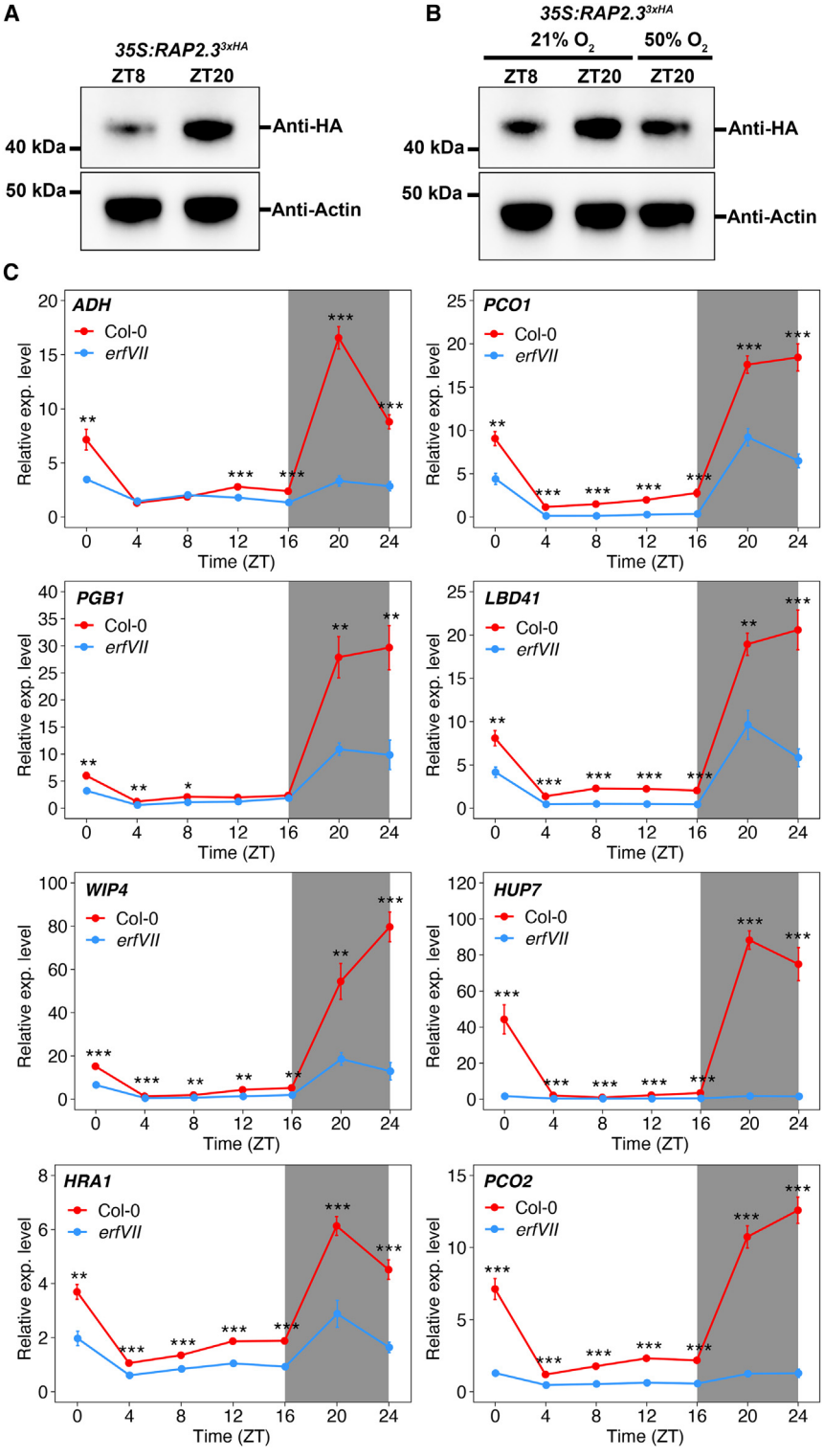

Figure 3. Cyclic hypoxia is an ERFVII-dependent response.

(A) Western blot analysis of RAP2.3^{3xHA} abundance at ZT8 and ZT20 under LD.

(B) Western blot analysis showing relative abundance of RAP2.3^{3xHA} at ZT8 and ZT20 under normoxia and at ZT20 under hyperoxia. Hyperoxia treatment started at the beginning of the night (ZT16).

(C) Gene expression analysis of hypoxia-responsive genes *ADH*, *PCO1*, *PGB1*, *LBD41*, *WIP4*, *HUP7*, *HRA1*, and *PCO2* in a time-course experiment using 7-day-old *Arabidopsis* Col-0 and *erfVII* mutant seedlings. Samples were collected every 4 h. The mRNA levels of genes were measured by RT–qPCR, and the data on the y-axis are expressed relative to Col-0 at ZT4 (ZT4 = 1). The x-axis shows zeitgeber time (ZT0, time when the lights are switched on). Data represent the mean ± SE of six biological replicates. Student's *t*-test was performed, and asterisks indicate statistically significant differences between Col-0 and *erfVII* mutant at each time point (*$P < 0.05$, **$P < 0.01$, ***$P < 0.001$).

energy shortage thus potentially involving the energy sensor TOR in cyclic hypoxia responses. Interestingly, inhibition of TOR by AZD-8055 treatment led to downregulation of *pPGB1:LUC* and *pPCO1:-LUC* activities in the night (supplemental Figure 14).

Treatment with DCMU at the beginning of the day impaired cyclic hypoxia responses antagonizing the downregulation of *pPGB1:LUC* and *pPCO1:LUC* typically observed in the daytime (Figure 4E). Moreover, *pPGB1:LUC* and *pPCO1:LUC* were upregulated by DCMU treatment under CL (supplemental Figure 15A). RAP2.3^{3xHA} was stabilized after 4 h of DCMU treatment under CL (supplemental Figure 15B) and DCMU treatment failed to induce cHRGs in *erfVII* mutant at the same level of wild-type under CL (supplemental Figure 15C).

Together, these findings suggest that the concerted action of photosynthesis and cellular respiration are responsible for the internal oxygen dynamics occurring under day/night cycles in actively growing young leaves.

Disruption of cyclic hypoxia impairs cellular respiration and starch breakdown altering shoot growth

To assess the impact of cyclic hypoxia on plant growth, we manipulated oxygen levels during the night by subjecting plants to hyperoxia or hypoxia treatments (Figure 5A). Hyperoxia treatment significantly reduced the activation of cHRGs, while hypoxia treatment strongly induced anaerobic gene expression (Figure 5B and 5C and supplemental Figure 16).

To evaluate the effect of disrupting cyclic hypoxia on shoot growth, these treatments were repeated for five consecutive nights (Figure 5D), and two key parameters of shoot growth, leaf number and area of young emerging leaves, were measured at the end of the treatment period (Figure 5E). Prolonged exposure

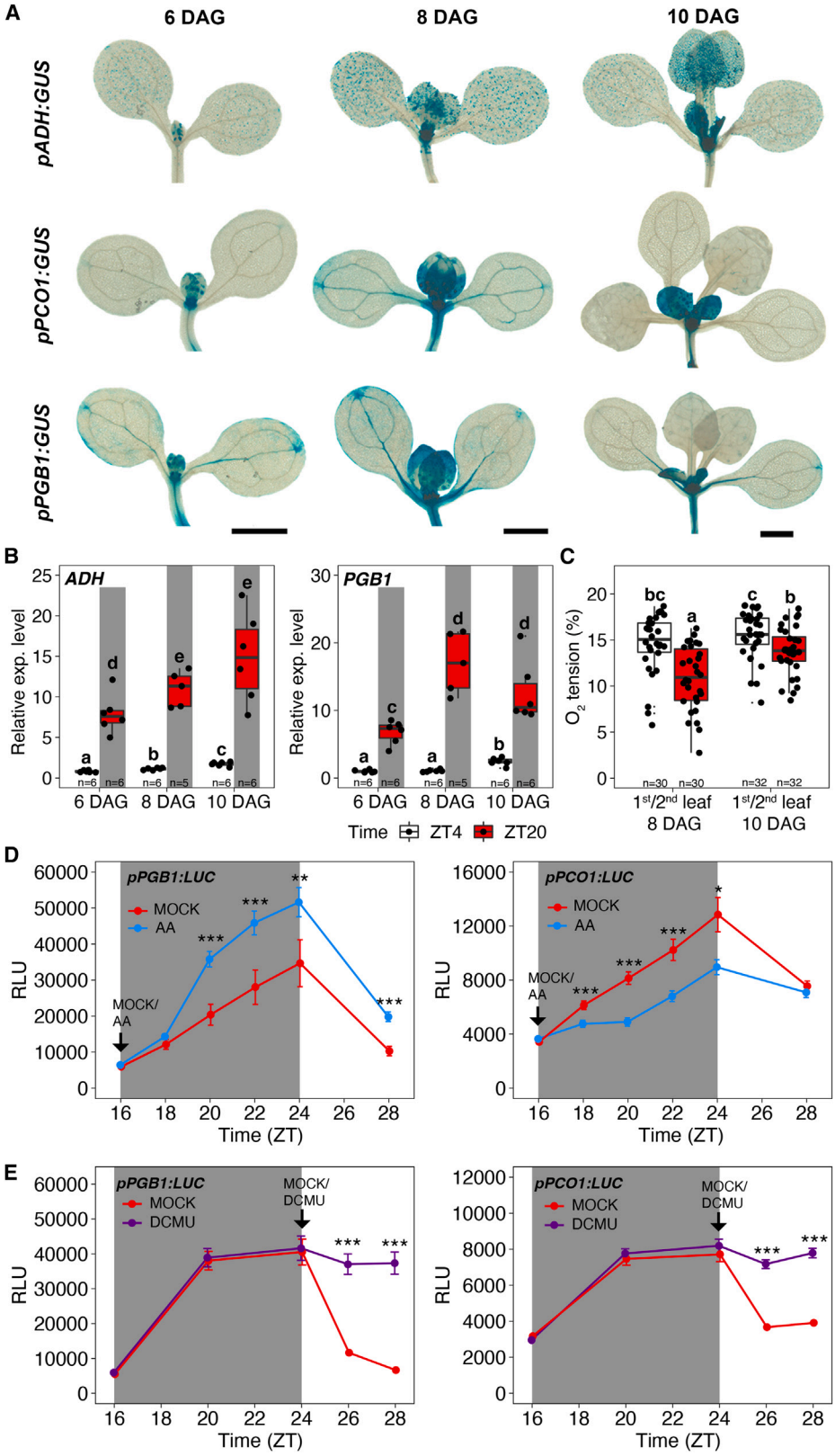

Figure 4. Concerted action of cellular respiration and photosynthesis generates cyclic hypoxia responses in young emerging leaves.
(A) Transgenic lines expressing the GUS gene under the control of the *ADH*, *PCO1*, and *PGB1* promoters (*pADH:GUS*, *pPCO1:GUS*, and *pPGB1:GUS*). GUS staining was performed after harvesting seedlings at the end of the night at 6, 8, and 10 days after germination (DAG). Scale bar corresponds to 1 mm.

(legend continued on next page)

to hyperoxia during the night led to a significantly higher leaf initiation rate and increased leaf area (Figure 5F and 5G), whereas hypoxia treatment resulted in reduced leaf number and area compared with the control (Figure 5H and 5I).

These findings indicate that eliminating cyclic hypoxia by providing external hyperoxia enhances shoot growth, while hypoxia strongly inhibits it. A higher external oxygen concentration would allow for a higher cellular respiration rate in young leaves during the night, leading to enhanced mobilization of starch and ATP production, thereby promoting leaf growth at night. Indeed, prolonged exposure to nocturnal hyperoxia failed to increase leaf number and area compared with the normoxia in the starchless *pgm* mutant (supplemental Figure 17). In line with these findings, gene expression analysis of *DIN6* showed higher induction in hyperoxia compared with normoxia at the end of the night, while hypoxia treatment inhibited its activation (supplemental Figure 18A). Moreover, *DIN6* gene expression was dramatically increased during the night and remained high during the early part of the daytime in the *erfVII* mutant compared with Col-0, as observed in the 24-h time-course experiment (supplemental Figure 18B).

Consistent with gene expression data, staining of starch confirmed that it is primarily degraded in young emerging leaves during a normoxic night, while nocturnal hypoxia and hyperoxia slows down and accelerates starch breakdown, respectively (supplemental Figure 19A and 19B). In the *erfVII* mutant, starch is degraded in young leaves and cotyledons at a much faster rate compared with the control, as evidenced by almost complete absence of Lugol staining during the night (supplemental Figure 19A and 19B).

To evaluate the metabolic activity depending on the time of the day in a tissue-specific manner, we performed fluorescence lifetime imaging (FLIM) to quantify NAD(P)H lifetime in cytoplasmic regions of epidermal cells as a proxy of cellular respiration rate in young emerging leaves (Figure 6). According to a well-established interpretation (Ferri et al., 2020; Azzarello et al., 2022), a change in NAD(P)H fluorescence lifetime reflects variations in cellular metabolism, either toward oxidative metabolism (i.e., with an increase in average lifetime) or toward glycolytic metabolism (i.e., with a decrease in average lifetime). Pixel-based analysis (Figure 6A) reveals that average NAD(P)H lifetime was significantly higher at ZT4 than at ZT20 in normoxia (Figure 6B). Conversely, the lowest NAD(P)H lifetime value was detected under hypoxia in the night, whereas hyperoxia increased NAD(P)H lifetime at ZT20, with a similar level observed at ZT4 (Figure 6B), indicating an oxygen-dependent decrease of oxidative phosphorylation (OXPHOS) in favor of glycolysis in the dark, which was attenuated by hyperoxia. Moreover, NAD(P)H lifetime was significantly higher in the *erfVII* mutant compared with Col-0 at ZT20 under normoxia (Figure 6B). Thus, ERFVIIs are required to promote the shift from OXPHOS to glycolysis in the dark. Phasor analysis (a technique to find the steady-state response when the system input is a sinusoid; Figure 6C) allows defining a metabolic trajectory that connects pixels with lifetime closer to the free form of NAD(P)H, with the enzyme-bound forms having longer lifetimes. The distributions of free NAD(P)H (Figure 6D) along the metabolic trajectory confirm the trend described above for all the conditions tested, as can be observed qualitatively in the metabolic maps (Figure 6E), in which cytoplasmic pixels are colored according to their different mixtures of free and bound NAD(P)H.

Collectively, our data suggest that cellular respiration and subsequent starch breakdown during the night are influenced by oxygen availability, and that this process is mediated by the action of ERFVIIs. Therefore, cyclic hypoxia plays a crucial role in regulating shoot growth during the night by determining the rate of starch degradation through the action of ERFVIIs.

ERFVII-dependent adaptation to cyclic hypoxia is required for shoot growth

During plant development, young emerging leaves experience a daily drop in oxygen level in the night, which triggers an ERFVII-dependent metabolic shift in young emerging leaves. Thus, we tested whether the absence of this metabolic switch occurring in young leaves in the night was detrimental for shoot growth and development. For this purpose, we compared shoot growth in Col-0 and *erfVII* mutant using a phenotyping system described previously (Ventura et al., 2020). In the early phases of shoot development, *erfVII* mutant plants showed significantly lower plant leaf area (PLA) and leaf number with respect to the wild-type under LD (Figure 7A and 7B). This result suggests that the lack of ERFVII-dependent adaptation to cyclic hypoxia in young leaves impairs shoot growth and development under LD. However, under CL, induction of *DIN6* as well as the cHRGs *ADH* and *PCO1* occurring under LD was abolished in both Col-0 and *erfVII* mutant (supplemental Figure 20), thus releasing the plant from the dependence of achieving cyclic hypoxia adaptation in young leaves. Moreover, gene expression of cell proliferation and expansion markers was significantly lower at the end of the night (ZT24) in *erfVII* mutant with respect to Col-0 under LD, but it was

(B) Gene expression analysis of *ADH* and *PGB1* in the shoot of the seedling at 6, 8, and 10 DAG under LD. The mRNA levels of genes were measured by RT–qPCR, and the data on the y-axis are expressed relative to ZT4 at 6 DAG (ZT4 at 6 DAG = 1). To calculate statistical significance, the Kruskal–Wallis test followed by post-hoc Wilcoxon test was carried out, and groups with significant differences ($P < 0.05$) are indicated with different letters (number of replicates is shown in the figure). Boxplots center line, median. The box extends from the 25th to 75th percentiles; whiskers, 1.5 interquartile range. Points out of the whiskers, outliers.

(C) Oxygen tension was measured using an oxygen microsensor probe at ZT4 and ZT20 in the first two young leaves at 8 DAG and on the same leaves at 10 DAG in *Arabidopsis* Col-0 seedlings. Data were analyzed with the Kruskal–Wallis test followed by post-hoc Wilcoxon test, and groups with significant differences ($P < 0.05$) are indicated with different letters. Boxplots center line, median. The box extends from the 25th to 75th percentiles; whiskers, 1.5 interquartile range. Points out of the whiskers, outliers.

(D) Luciferase activity of *pPGB1:LUC* and *pPCO1:LUC* seedlings (9 days old) detected by luminescence assay from ZT16 to ZT28 after MOCK (EtOH) or AA treatments were applied at ZT16 (indicated by the black arrow) under LD. The data represent the mean ± SE (*pPGB1:LUC*_MOCK, $n = 32$; *pPGB1:LUC*_AA, $n = 33$; *pPCO1:LUC*_MOCK, $n = 32$; *pPCO1:LUC*_AA, $n = 38$).

(E) Luciferase activity of *pPGB1:LUC* and *pPCO1:LUC* seedlings (9 days old) detected by luminescence assay from ZT16 to ZT28. MOCK (DMSO) or DCMU treatments were applied at ZT24 (indicated by the black arrow) under LD. The data represent the mean ± SE (*pPGB1:LUC*_MOCK, $n = 35$; *pPGB1:LUC*_DCMU, $n = 35$; *pPCO1:LUC*_MOCK, $n = 38$; *pPCO1:LUC*_DCMU, $n = 36$).

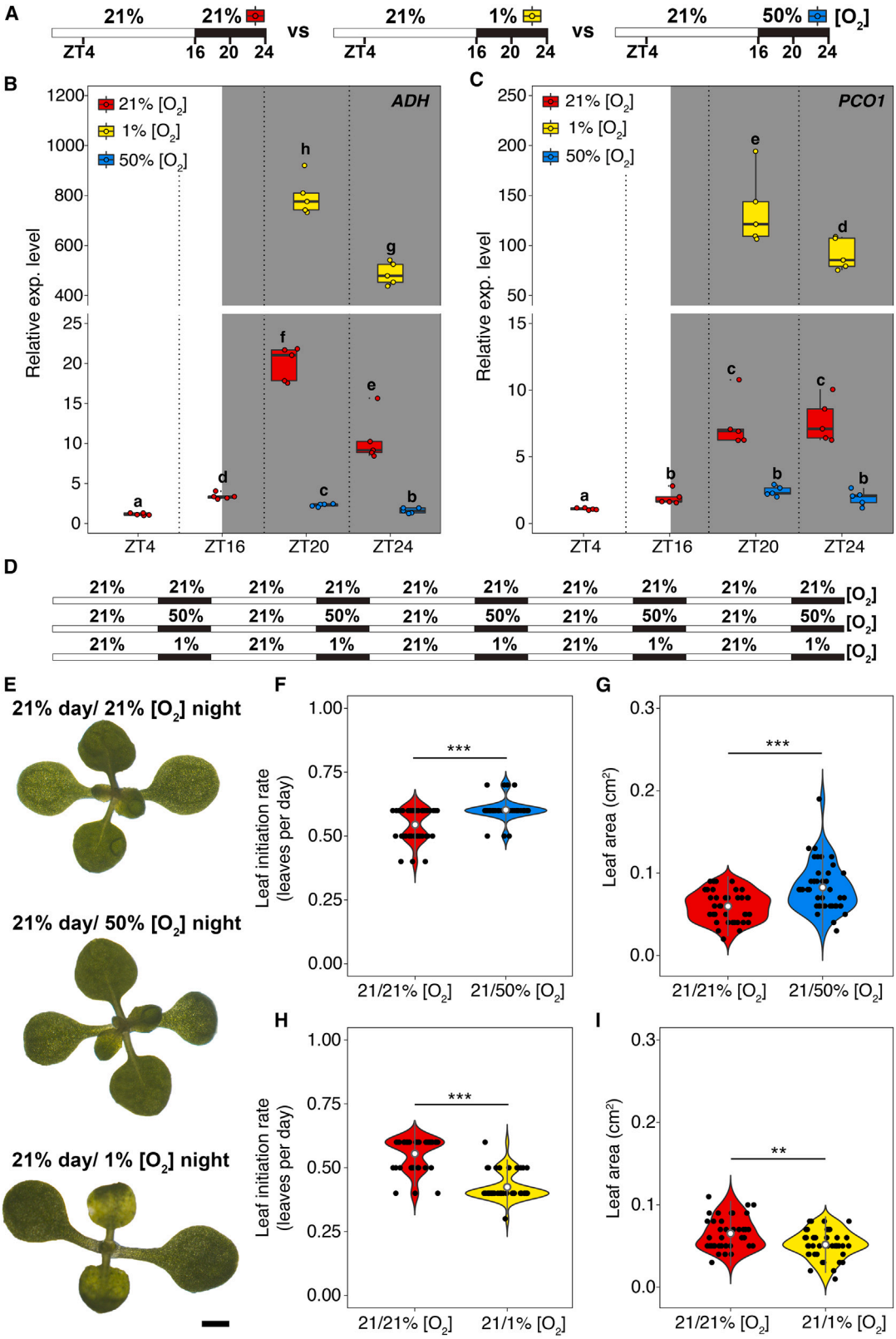

Figure 5. Disrupting cyclic hypoxia alters shoot growth.

(A) The experimental setup showing different conditions and time points of sample collection.

(B and C) Gene expression analysis of *ADH* and *PCO1* at ZT4, 16, 20, and 24 in 8-day-old *Arabidopsis* Col-0 shoots under LD, where the night was kept at normoxia, hypoxia, or hyperoxia. Dotted lines separate different time points. The mRNA levels of genes were measured by RT–qPCR, and the data on the

(legend continued on next page)

unchanged at ZT24 under CL at least for *CYCB1*;*1*, *CYCD3*;*1*, and *EXP1* genes (supplemental Figure 21).

Therefore, we evaluated shoot growth of Col-0 and *erfVII* mutant under CL conditions. At similar developmental stages, there were no significant differences in PLA and leaf number between Col-0 and the *erfVII* mutant under CL (Figure 7C and 7D). The recovery of *erfVII* shoot growth under CL indicates that the ERFVII-dependent adaptation to cyclic hypoxia, which is crucial under light/dark cycles, is no longer necessary when cyclic hypoxia is eliminated. Similarly, the *adh* mutant, where ADH enzyme is missing, showed significantly lower PLA and leaf number Col-0 under LD but not under CL (supplemental Figure 22). Thus, ERFVII-dependent cyclic hypoxia responses play a crucial role in controlling shoot growth under day/night cycles.

DISCUSSION

When plants experience hypoxia, which can be caused by a specific environmental or physiological condition, their metabolism undergoes a readjustment through a drastic modulation of gene expression (Mustroph et al., 2010). This transcriptional reprogramming is orchestrated by ERFVII transcription factors, which are PCO N-degron pathway substrates (Licausi et al., 2011b; Gibbs et al., 2011). ERFVII stability and action is mediated by oxygen and NO (Gibbs et al., 2014; Weits et al., 2014; Hartman et al., 2019; Zubrycka et al., 2023). By sensing atmospheric oxygen concentrations, ERFVIIs are also part of a genetic mechanism required for adaptation to altitude in angiosperms (Abbas et al., 2022). Furthermore, the discovery of chronic hypoxic niches in the meristem regions of the plant, in which the novel substrates ZPR2 and VRN2 of the PRT6 N-degron pathway participate, has expanded the implication of the oxygen-sensing mechanism to several plant developmental processes (Shukla et al., 2019; Weits et al., 2019; Labandera et al., 2021).

While these studies have shed light on the events upstream of oxygen-dependent gene regulation, little is known about spatio-temporal dynamics of oxygen concentration in the plant and about how oxygen sensing allows the fine-tuning of diurnally generated internal oxygen gradients with plant growth and metabolism. In contrast, the study of temporal oxygen dynamics in the context of cancer research has recently received considerable attention, leading to the definition of cyclic hypoxia (Bader et al., 2020).

The temporal fluctuations of oxygen levels in tumor tissues are monitored by an analogous oxygen-sensing pathway described for plants (Holdsworth and Gibbs, 2020; Licausi et al., 2020). Given this similarity, it is tempting to speculate that, if temporal oxygen fluctuations occur within the plant body, daily changes in the gene expression of HRGs ought to be observed. In fact, our data showed that expression of HRGs as well as transcriptional activation of hypoxia-responsive reporters display diurnal patterns and are activated at night (Figure 1), thus demonstrating the existence of cyclic hypoxia in plants. Since CL eliminated the nocturnal activation of cHRGs, we ruled out the direct regulation of circadian clock on cyclic hypoxia (Figure 2), although an interplay between the molecular clock and cyclic hypoxia might exist.

Nocturnal hyperoxia treatment dampened cHRG gene expression (Figure 2), suggesting that cyclic hypoxia was the result of an internal oxygen drop. RAP2.3^{3xHA} was stabilized in the night, whereas nocturnal hyperoxia led to its destabilization at ZT20 although not with the same degree observed in the daytime. Accordingly, RAP2.3^{3xHA} becomes stable in the dark at 21% of ambient oxygen when compared with the control condition in the light (Zubrycka et al., 2023). Consistent with diurnal-dependent ERFVII stability, the gene expression of cHRGs in the pentuple mutant *erfVII* was significantly reduced or totally abolished (Figure 3).

However, some cHRGs still showed partial activation in *erfVII* in the nighttime (Figure 3), indicating that other factors could contribute to cyclic hypoxia. Analysis of cHRGs in both *prt6* and *ate1ate2* mutants, where PRT6 N-degron substrates are constitutively stabilized (Licausi et al., 2011b; Gibbs et al., 2011), showed that they were activated in the night (supplemental Figure 5), suggesting the existence of alternative pathways to the PRT6 N-degron, which could participate in the establishment of cyclic hypoxia responses.

In addition to ERFVII-responsive motifs, other transcription factor-DNA binding sites have been found in the promoters of HRGs (Gasch et al., 2016) and it has been recently reported that NO APICAL MERISTEM/ARABIDOPSIS TRANSCRIPTION ACTIVATION FACTOR/CUP-SHAPED COTYLEDON (NAC) transcription factors, including ANAC013 and ANAC017, bind to the mitochondrial dysfunction motif (MDM) located in the promoters of multiple HRGs, thus activating their gene expression during hypoxia (De Clercq et al., 2013; Eysholdt-Derzsó et al., 2023). Among these HRGs, *ADH*, *PGB1*, and *LBD41*, which showed an activation, although limited, of gene expression in the night in *erfVII* mutant, presented MDMs in their promoters. Thus, it can be speculated that ANAC013 as well as ANAC017 contribute to the control of cyclic hypoxia responses in addition to ERFVIIs.

ERFVII stability is also controlled by NO (Gibbs et al., 2014; Hartman et al., 2019). NO endogenous levels mainly depend on nitrate

y-axis are expressed relative to ZT4 (ZT4 = 1). To calculate statistical significance, the Kruskal–Wallis test followed by the post-hoc Wilcoxon test was carried out, and groups with significant differences ($P < 0.05$) are indicated with different letters. Boxplots show the center line as the median; the box extends from the 25th to 75th percentiles; whiskers represent 1.5 interquartile range; points outside the whiskers are outliers ($n = 5$ biological replicates).
(D) The experimental setup showing the treatment performed for 5 consecutive nights.
(E) Representative pictures of 10-day-old *Arabidopsis* Col-0 seedlings after 5 days of growing under normoxia in the daytime and under normoxia, hypoxia, or hyperoxia during the night.
(F and G) Quantification of leaf initiation rate and true leaf area in *Arabidopsis* Col-0 seedlings after prolonged hyperoxic treatment in the night ($n = 42$) compared with the normoxic condition ($n = 41$).
(H and I) Quantification of leaf initiation rate and true leaf area in *Arabidopsis* Col-0 seedlings after prolonged hypoxic treatment in the night ($n = 41$) compared with the normoxic condition ($n = 38$). Data were analyzed with the Kruskal–Wallis test. Asterisks represent statistically significant differences between the different conditions (**$P < 0.01$, ***$P < 0.001$). Violin plots depict the density of data, where the width of the colored area illustrates the proportion of the data with a specific score. White dots and middle gray bars show the mean and standard deviation, respectively.

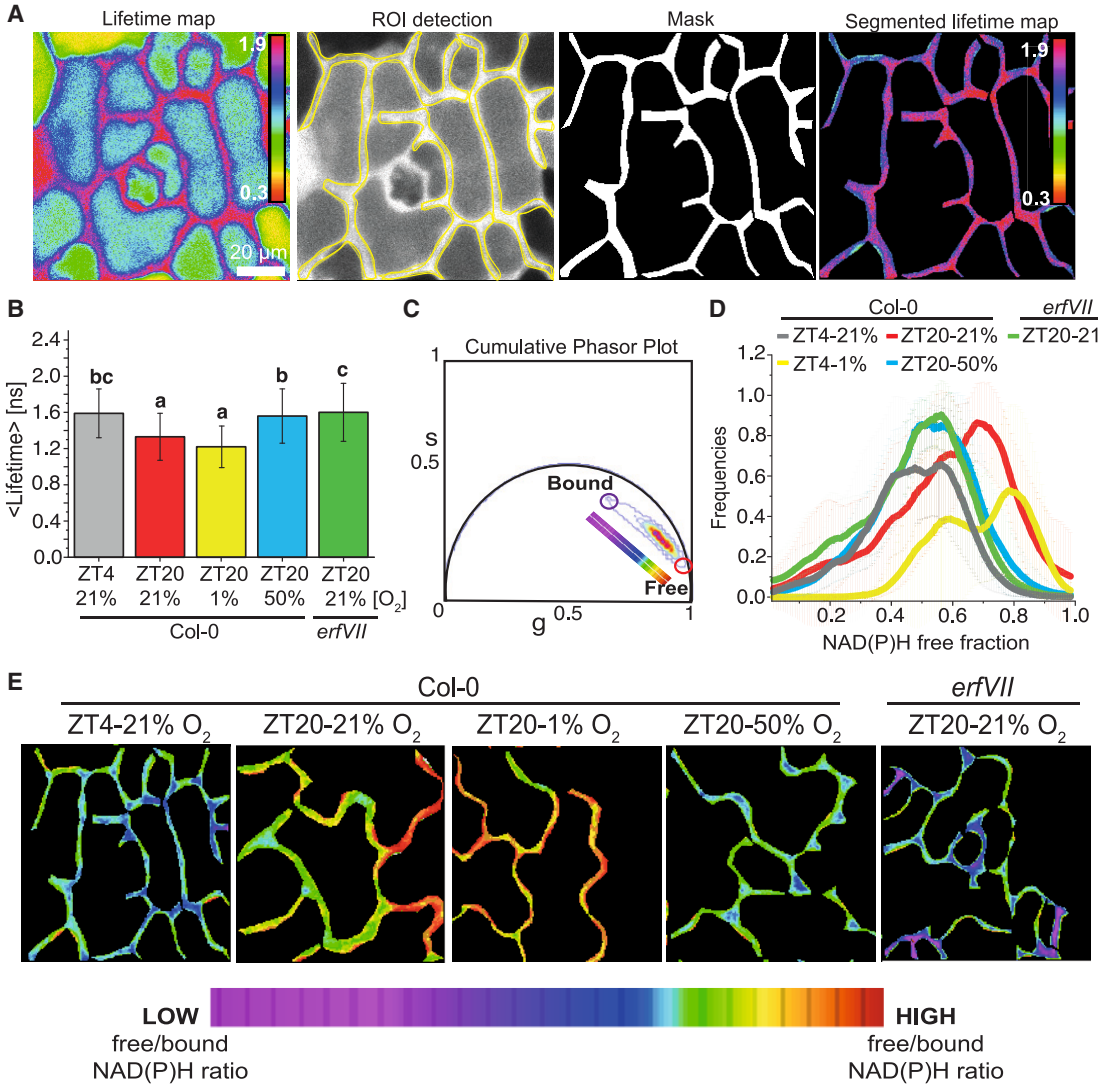

Figure 6. Tissue-specific fluorescence NAD(P)H lifetime imaging reveals a metabolic shift from oxidative phosphorylation to glycolysis at night in young emerging leaves.

(A) Workflow of NAD(P)H lifetime analysis. Acquired NAD(P)H lifetime maps were segmented to isolate cytoplasmic regions and extract the first moment of the photon lifetime distribution measured in each pixel, i.e., the average lifetime value (in nanoseconds) observed in that pixel, colored according to the color bar depicted in figure.

(B) Averages and standard deviations of lifetime values for each measured condition. Kruskal–Wallis test was used to determine the statistical significance of the differences observed (n = 10). Groups with significant differences (P < 0.001) are indicated with different letters.

(C) Cumulative phasor plot of NAD(P)H lifetimes. Violet and red circles define the higher lifetime values in the phasor plot characteristic of enzyme-bound NAD(P)H and the lower lifetime values characteristic of free NAD(P)H, respectively.

(D) Normalized frequencies of NAD(P)H free fraction (1 = 100% of NAD(P)H free fraction) extracted from phasor analysis for each acquisition, represented as mean values and standard deviations for each condition.

(E) Metabolic map of the cytoplasmic regions of representative acquisitions of the five conditions tested. The applied color bar spans from the lower free/bound NAD(P)H ratio region of the phasor in **(C)** (violet) to the highest free/bound ratio in red.

reductase activity in plants, which is low at night and increases during the first hours of the day (Pilgrim et al., 1993). Thus, lower NO levels in the night in young emerging leaves could contribute to ERFVII stability and cyclic hypoxia, whereas increasing NO levels in the morning would lead to ERFVII degradation dampening cyclic hypoxia responses. By altering either genetically or chemically endogenous NO levels (supplemental Figure 6), we provide evidence that, although NO endogenous fluctuations could contribute to cyclic hypoxia, oxygen levels appear to be largely prevailing to define the oscillations in cHRGs expression.

ERFVIIs also repress tetrapyrrole synthesis gene expression and chlorophyll biosynthesis (Abbas et al., 2015, 2022). Remarkably, among them, protochlorophyllide oxidoreductase (*POR*)*A*, *PORB*, and *PORC*, which catalyze the photoreduction of protochlorophyllide to chlorophyllide, show circadian and diurnal regulation, and are activated in the daytime in mature leaves (Matsumoto et al., 2004). Whether ERFVIIs control diurnal tetrapyrrole synthesis gene expression in the context of cyclic hypoxia remains to be determined. Oxygen sensing through diurnally controlled ERFVII stability and action may fine-tune tetrapyrrole

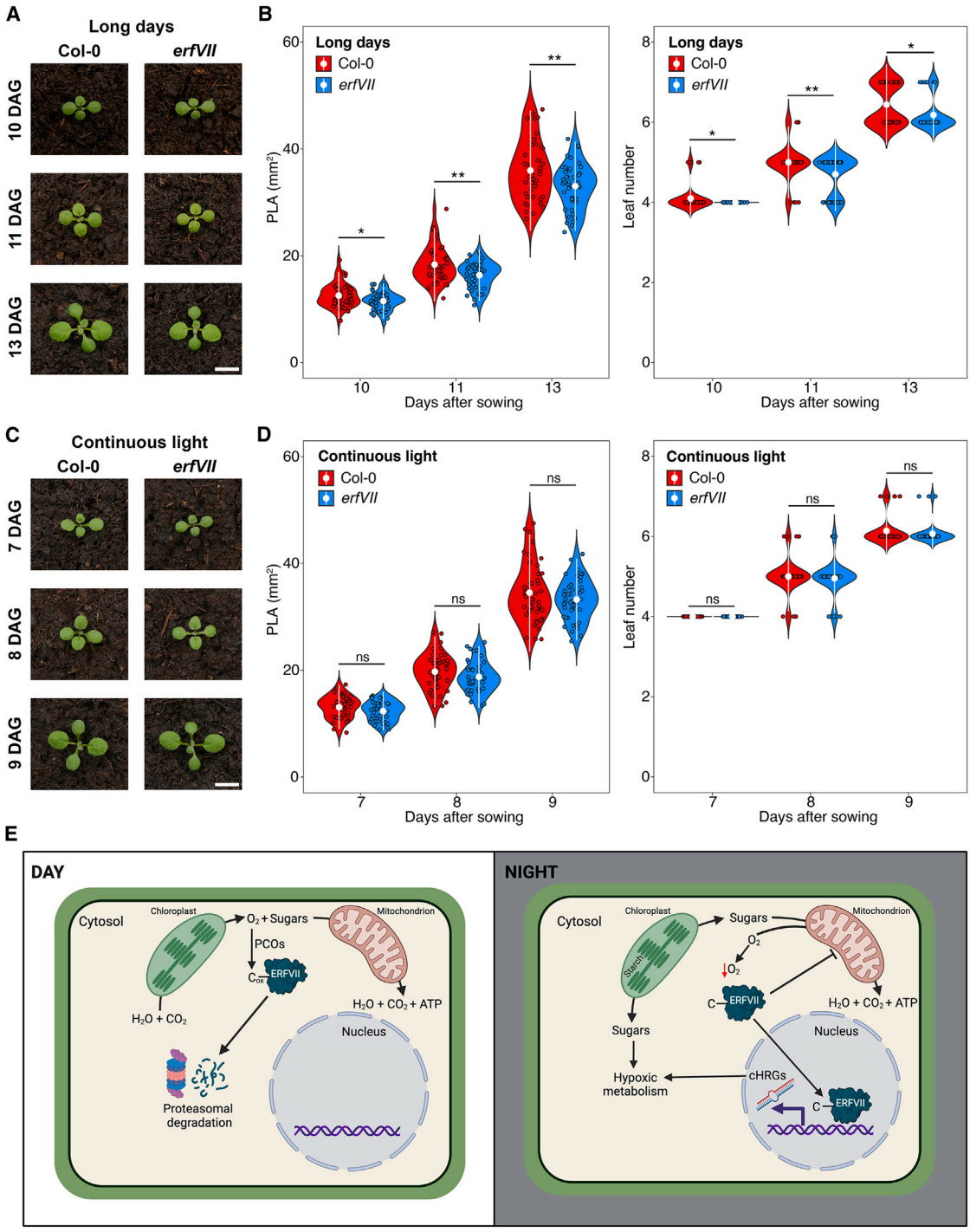

Figure 7. ERFVII-dependent mechanism is required for daily cyclic hypoxia adaptation in young emerging leaves.

(A) Representative picture of *Arabidopsis* Col-0 and *erfVII* mutant plants at 10, 11, and 13 DAG grown under LD conditions. Scale bar corresponds to 2 cm.

(B) Quantification of plant leaf area (PLA) and leaf number at 10, 11, and 13 DAG under LD in Col-0 ($n = 41$) and *erfVII* mutant ($n = 44$) plants. Leaf area was analyzed with one-way ANOVA, while leaf number was analyzed with Kruskal–Wallis test. Asterisks represent statistically significant differences between Col-0 and *erfVII* mutant for each time point (ns, not significant; $^{*}P < 0.05$, $^{**}P < 0.01$). Violin plots depict the density of data, where the width of the colored area illustrates the proportion of the data with a specific score. White dots and bars show the mean and standard deviation, respectively.

(C) Representative picture of *Arabidopsis* Col-0 and *erfVII* mutant plants at 7, 8, and 9 DAG grown under CL conditions. Scale bar corresponds to 2 cm.

(D) Quantification of PLA and leaf number at 7, 8, and 9 DAG under CL in Col-0 ($n = 44$) and *erfVII* mutant ($n = 44$) plants. Leaf area was analyzed with one-way ANOVA test, while leaf number was analyzed with Kruskal–Wallis test. Asterisks represent statistically significant differences between Col-0 and *erfVII* mutant for each time point (ns, not significant; $^{*}P < 0.05$, $^{**}P < 0.01$). Violin plots depict the density of data, where the width of the colored area illustrates the proportion of the data with a specific score. White dots and bars show the mean and standard deviation, respectively.

(legend continued on next page)

synthesis gene expression with cyclic oxygen levels avoiding accumulation of highly photoreactive chlorophyll intermediates and preventing photodamage upon illumination in young leaves (Tian et al., 2021).

Gene expression analyses, along with evaluation of hypoxia-responsive GUS and LUC reporter lines revealed that cyclic hypoxia primarily occurs in the young emerging leaves (Figure 4, supplemental Figures 8–11, and supplemental Videos 1 and 2). Furthermore, internal oxygen levels measurements using a micro Clark-type O_2 electrode at different stages of leaf development and time of the day, showed that young emerging leaves experience mild hypoxia (~10% [O_2]) in the night (Figure 4C), thus demonstrating that temporal oxygen dynamics occurred in the young emerging leaves. These findings strongly support the existence of cyclic hypoxia and highlight the importance of light/dark cycles, especially for actively growing photosynthetic tissues, in the generation of temporal oxygen dynamics.

Interestingly, RELATED TO APETALA 2.12 (RAP2.12), a member of ERFVIIs, and ANAC013 started to translocate to the nucleus of cells at 10% and 8% O_2, respectively (Kosmacz et al., 2015; Eysholdt-Derzsó et al., 2023). Moreover, moderate decrease of [O_2] (from 21% to 8%) was sufficient to activate the gene expression of 12 mild-HRGs (Van Dongen et al., 2009). Among these genes, *ADH*, *PCO1*, *PGB1*, *WIP4*, *HRA1*, and *LBD41* were found to be upregulated at 8% O_2. Consequently, in this study all these HRGs together with *HUP7* and *PCO2* were identified as cHRGs. The fact that only a portion of HRGs is sensitive to mild hypoxia could be explained by either a different intrinsic responsiveness of their promoters to ERFVIIs and/or by the action of additional transcriptional activators that trigger the induction of this set of mild hypoxia-sensitive genes.

Based on our experimental evidence, we propose that the internal drop of oxygen is caused by the high respiration rate required to support energy production in the actively growing leaves. Treatment with AA, which blocks the activity of the mitochondrial complex III and inhibits oxygen consumption (Kalbáčová et al., 2003), significantly reduced the activation of *pPCO1:LUC* in the night and gene expression of cHRGs at ZT20 (Figure 4 and supplemental Figure 12). However, both *pPGB1:LUC* and *PGB1* gene expression were activated by AA, while *LBD41* expression was unchanged (Figure 4 and supplemental Figure 12). Both *PGB1* and *LBD41* contain at least one MDM. In addition, AA triggers migration of ANAC013 to the nucleus in aerobic conditions (Eysholdt-Derzsó et al., 2023). Both reducing *ANAC013* gene expression, and impairment of its nuclear translocation-reduced activation of *LBD41* gene expression, whereas mutations on MDM sites within the *PGB1* promoter reduced its ANAC013-dependent activation (Eysholdt-Derzsó et al., 2023). Thus, the different regulation displayed by cHRGs after AA treatment could be the result of the cross-action of different oxygen-related pathways and/or regulatory events occurring with different temporal dynamics.

Besides the inhibition of oxygen consumption, NO production is induced in tobacco leaves after AA treatment (Alber et al., 2017). Thus, *PGB1* activation by AA could contribute to the NO scavenging and thus stabilizing ERFVIIs, which in turn would activate HRGs. However, AA-induced NO production occurs in concomitance with reduction of oxygen consumption in mitochondria, thus cHRGs activation could be uncoupled under this condition. Consistent with *PGB1* activation, HYPOXIA-RESPONSIVE ERF2 (HRE2), a member of the ERFVII group, is clearly stabilized after 5 h of AA treatment (Barreto et al., 2022). However, we found that AA treatment represses 6 out of 8 cHRGs within 4 h in the night, being effective after 2 h on *pPCO1:LUC* activity (Figure 4). It remains unknown whether ERFVIIs stabilization by AA translates into the activation of HRGs. It is possible that upon mitochondrial dysfunction, despite the stabilization of ERFVIIs, ATP depletion caused by the drop of ATP synthase activity (Wagner et al., 2018) is sensed by the TOR complex, which in turn modulates the activity of ERFVIIs and hypoxia-dependent transcriptional responses according to energy availability (Kunkowska et al., 2023). Indeed, either carbon starvation or TOR inhibition significantly reduced activation of cHRGs and *pPGB1:LUC* and *pPCO1:LUC* in the night, respectively (supplemental Figures 13 and 14). Therefore, carbon shortage could affect gene expression of cHRGs by either reducing the rate of cellular respiration leading to a reduction of O_2 consumption and/or by compromising the energy status of the cells and TOR activity, which in turn regulates the magnitude of the induction of cHRGs by modulating ERFVII activity.

Photosynthetic oxygen evolution is essential to downregulate *pPGB1:LUC* and *pPCO1:LUC* in the morning and to prevent induction of cHRGs, *pPGB1:LUC* and *pPCO1:LUC*, under CL (Figure 4 and supplemental Figure 15). Importantly, this activation is an ERFVII-dependent response (supplemental Figure 15). Thus, resumption and maintenance of proper photosynthetic activity is essential to both dampen and prevent ERFVII-dependent cyclic hypoxia responses in young leaves during the daytime. Interestingly, N-degron pathway enzymes, particularly *MAP2A* and *PCO5*, are upregulated at the end of the night (supplemental Figure 7), suggesting a diurnal coordination between the first steps of ERFVII destabilization and the increase of endogenous oxygen levels in the morning.

Prolonged nocturnal hyperoxia or hypoxia treatments promote or inhibit leaf growth, respectively (Figure 5). Nocturnal hyperoxia triggered higher gene expression of the carbon starvation marker *DIN6*, while hypoxia led to a reduction in *DIN6* expression compared with normoxia at the end of the night (supplemental

(E) A working model (created with BioRender.com) showing the role of cyclic hypoxia in young leaves. During daytime, photosynthetic activity provides sugars and oxygen, which are the substrates of cellular respiration. This metabolic pathway ensures energy supplies to sustain growth in actively growing young leaves. Oxygen availability also leads to the PCO-dependent oxidation of cysteine (C_{ox}) at the N terminus of ERFVIIs, triggering their degradation via the N-degron pathway during the daytime. However, at night, oxygen provision relies on the gas diffusion, while starch is the main source of sugars for cellular respiration. In these conditions, the high respiration rate leads to a temporary fall (red arrow) in endogenous oxygen levels that triggers ERFVII-dependent hypoxia transcriptional responses. Consequently, ERFVIIs act both as repressors and activators of aerobic and hypoxic metabolism, respectively. This ERFVII-dependent metabolic balance enables the modulation of leaf growth according to the availability of carbon sources and oxygen in actively growing leaves. Arrows and lines indicate promoting and inhibiting effects, respectively.

Figure 18). Although *DIN6* expression was previously found to be activated by an extended submergence/hypoxia treatment, its induction was antagonized by addition of exogenous sugars, indicating that *DIN6* activation by hypoxia was a consequence of carbon starvation (Baena-González et al., 2007). Staining for spatial starch distribution revealed a lower starch content after nocturnal hyperoxia, whereas it was higher after hypoxia compared with normoxia in the young emerging leaves (supplemental Figure 19). Hyperoxia treatment during the night was able to restore adequate internal oxygen levels, which, in turn, sustains the respiration rate and leads to more rapid starch breakdown and leaf growth. Nocturnal hyperoxia treatment on the starchless mutant *pgm* failed to promote shoot growth (supplemental Figure 17), indicating that the positive effect of hyperoxia treatment on leaf growth requires starch as a substrate fueling cellular respiration. Interestingly, the *erfVII* mutant exhibited a strong induction of *DIN6* and accelerated consumption of starch at night (supplemental Figures 18 and 19). This result was in line with the previously proposed function of RAP2.12 and RAP2.2, both acting as a repressors of cellular respiration in favor of the activation of fermentative pathways (Paul et al., 2016; Tsai et al., 2023). Indeed, *DIN6* was downregulated in the presence of the constitutively stable version of RAP2.12 during an extended night (Loreti et al., 2018), likely as a consequence of the slower rate of cellular respiration and starch breakdown. Therefore, temporal oxygen dynamics dictate the rate of cellular respiration and starch breakdown to fine-tune leaf growth based on oxygen availability. The rate of nocturnal starch degradation is controlled by a sophisticated, clock-related mechanism, allowing the plant to ensure that starch reserves are depleted at dawn (Smith and Zeeman, 2020). Our results indicate that cyclic hypoxia could contribute to this process in a clock-independent manner.

Fluorescence lifetime imaging of NAD(P)H in epidermal cells of young leaves confirmed that a metabolic shift exists from the daytime to the nighttime, and it depends on the oxygen concentration. In the daytime, OXPHOS, besides photosynthesis, is the main metabolic pathway providing energy to the cells (Figure 6). However, OXPHOS is reduced at night, and glycolysis predominates as a consequence of internal oxygen drop (Figure 6). Importantly, this metabolic shift is controlled by the ERFVIIs (Figure 6).

The stability of ERFVIIs would seem to create a competitive mechanism between aerobic and anaerobic pathways in the context of a mild hypoxia, setting the pace of carbon consumption in the young emerging leaves during the night.

When this ERFVII-dependent competitive mechanism is absent, leaf growth is negatively affected in the early phases of shoot development (Figure 7A and 7B). Consistently, lack of ADH negatively impacts shoot growth under day/night cycles (supplemental Figure 22). However, under CL, both cyclic hypoxia and carbon starvation are abolished and adaptation to cyclic hypoxia is no longer required (supplemental Figure 20). This is demonstrated by the absence of differences in shoot growth between wild-type and *erfVII* as well as *adh* mutant in the early stage of plant development (Figure 7C and 7D and supplemental Figure 22).

In conclusion, our findings demonstrate that the presence of an ERFVII-dependent mechanism is essential for the adaptation to cyclic hypoxia in young leaves, allowing for the precise adjustment of leaf growth in response to the carbon status and oxygen availability within plant cells. During the daytime, photosynthesis provides oxygen and sugars that sustain aerobic metabolism. At night, a moderate decrease in internal oxygen levels occurs in young emerging leaves, triggering the activation of cyclic HRGs through the action of ERFVIIs (Figure 7E). This molecular event represents a switch from aerobic to hypoxic metabolism, regulating the rate of starch consumption and plant growth according to the availability of internal oxygen. A functional connection thus exists between internal temporal oxygen dynamics and the developmental processes of plants.

METHODS

Plant materials and growth conditions

Arabidopsis thaliana Columbia-0 (Col-0) was used as the wild-type ecotype. *prt6* and *ate1ate2* knockout mutants were described previously (Licausi et al., 2011b). The pentuple *erfVII* mutant (Abbas et al., 2015) was kindly provided by Dr. Michael Holdsworth (University of Nottingham). *35S:RAP2.3*^{3xHA} line (Gibbs et al., 2014) was kindly provided by Dr. Sjon Hartman (University of Freiburg). *cue1-6* and *nia1nia2noa1-2* mutants (Streatfield et al., 1999; Lozano-Juste and León, 2010) were kindly provided by Dr. Oscar Lorenzo (University of Salamanca). Reporter lines *pPGB1:LUC* (Licausi et al., 2011a), *pADH:GUS* (Ventura et al., 2020), and *pPCO1:GUS* (Weits et al., 2014) were described previously.

Plant growth conditions are described in detailed in the supplemental experimental procedures.

Inhibitor and chemical treatments

AA (Sigma-Aldrich) and DCMU (Sigma-Aldrich) were applied at a concentration of 100 and 20 μM, respectively. For SNAP MedChemExpress) and cPTIO (Sigma-Aldrich) treatments, final concentrations of 300 and 200 μM were used, respectively. The mTOR inhibitor AZD-8055 (MedChem Express) was applied at a concentration of 5 μM.

Construct preparation

To generate *pPGB1:GUS* and *pPCO1:LUC* reporter lines, the *PGB1* and *PCO1* promoters (369 and 1131 bp upstream the transcriptional starting site, respectively), available in pENTR/D-TOPO entry vectors (Life Technologies), were recombined into pKGWFS7 and pBGWL7 destination vectors using the LR reaction mix II (Life Technologies) to obtain *pPGB1:GUS* and *pPCO1:LUC* constructs, respectively.

Procedure for generation of transgenic plants is described in detail in the supplemental experimental procedures.

Spatial detection of NO, GUS, and starch staining

Spatial distribution of endogenous NO was analyzed as described previously (Barreto et al., 2022). Histochemical GUS staining was carried out according to Jefferson et al. (1987). Qualitative assessment of starch distribution was performed by Lugol staining as described previously (Loreti et al., 2018). Extended protocols are provided in the supplemental experimental procedures.

Oxygen-modified atmosphere treatments and measurement

Hypoxic or hyperoxic treatments were performed using an enclosed anaerobic workstation (O2 Control InVitro Glove Box; Coy Laboratory Products) by flushing an oxygen-modified atmospheres (1% [v/v] O_2/N_2) or (50% [v/v] O_2) for hypoxia or hyperoxia, respectively. Oxygen concentration in young emerging leaves was measured using a FireStingO2 high-precision, PC-controlled fiber-optic oxygen meter (Pyro Science) and a detailed procedure is described in the supplemental experimental procedures.

Total RNA extraction and real-time qPCR analysis

Total RNA was extracted from *Arabidopsis* seedlings using a phenol–chloroform extraction protocol (Perata et al., 1997) and RNA assessment, cDNA synthesis and real-time quantitative PCR were performed as described in detail in Loreti et al. (2020). *UBIQUITIN10* (At4G05320) was used as the housekeeping gene for internal normalization and relative expression level was calculated using the $2^{-\Delta\Delta CT}$ method. A list of primers used for qPCR analyses is included in supplemental Table 2.

Protein extraction, SDS–PAGE, and immunoblotting analysis

Total protein extractions were obtained from shoots of 8-day-old *Arabidopsis* seedlings and western blots of ERVII stability were performed as described in the supplemental experimental procedures.

Luciferase activity quantification

To continuously monitor the luciferase activity of *pPGB1:LUC* and *pPCO1:LUC* reporter lines, the method described previously was followed (Ramos-Sánchez et al., 2017). *In vivo* luciferase activity imaging was carried out using the NightSHADE evo LB 985N In Vivo Plant Imaging System (Berthold Technologies, Germany). Detailed information about plant growth conditions and luminescence quantification are provided in the supplemental experimental procedures.

NAD(P)H FLIM

FLIM was performed on an Olympus Fluoview 3000 confocal microscope coupled with a lifetime imaging module from Picoquant. Intracellular NAD(P)H ("NAD(P)H" denotes both NADH and NADPH since the fluorescence properties of the nicotinamide ring of NADH and NADPH are identical; Blacker et al., 2014) was excited with a pulsed 375-nm laser set to 40 MHz of repetition rate (25 ns of decay-detection window), while the emission was collected on PMA hybrid detectors (Picoquant) in the 420–460-nm range. Processing of fluorescence lifetime imaging is described in the supplemental experimental procedures.

SUPPLEMENTAL INFORMATION

Supplemental information is available at *Molecular Plant Online*.

FUNDING

This work was supported by Sant'Anna School of Advanced Studies, Pisa (Italy). P.M.T. was awarded the Margarita Salas Post-Doc fellowship by the Universidad Politécnica de Madrid (Spain) and funded by European Union-NextGenerationEU (UP2021-035). We acknowledge the Italian Ministry of University and Research for funding the PINS project as part of the joint program "Le Scuole Superiori ad Ordinamento Speciale: istituzioni a servizio del Paese."

AUTHOR CONTRIBUTIONS

Conceptualization, P.M.T., E.L., M.P., and P.P.; methodology, P.M.T., L.B., G.N., G.F., F.C., E.L., M.P., and P.P.; investigation, P.M.T., L.B., G.N., G.F., and M.P.; writing – original draft, P.M.T., E.L., and P.P.; writing – review & editing, P.M.T., L.B., G.N., G.F., F.C., E.L., M.P., and P.P.; funding acquisition, P.M.T., F.C., E.L., and P.P.; resources, F.C., E.L., M.P., and P.P.; supervision, F.C., E.L., M.P., and P.P.

ACKNOWLEDGMENTS

The authors declare no competing interest.

Received: December 6, 2023
Revised: January 11, 2024
Accepted: January 15, 2024
Published: January 19, 2024

REFERENCES

Abbas, M., Berckhan, S., Rooney, D.J., Gibbs, D.J., Vicente Conde, J., Sousa Correia, C., Bassel, G.W., Marín-de la Rosa, N., León, J., Alabadí, D., et al. (2015). Oxygen Sensing Coordinates Photomorphogenesis to Facilitate Seedling Survival. Curr. Biol. **25**:1483–1488.

Abbas, M., Sharma, G., Dambire, C., Marquez, J., Alonso-Blanco, C., Proaño, K., and Holdsworth, M.J. (2022). An oxygen-sensing mechanism for angiosperm adaptation to altitude. Nature **606**:565–569.

Alber, N.A., Sivanesan, H., and Vanlerberghe, G.C. (2017). The occurrence and control of nitric oxide generation by the plant mitochondrial electron transport chain. Plant Cell Environ. **40**:1074–1085.

Azzarello, F., Pesce, L., De Lorenzi, V., Ferri, G., Tesi, M., Del Guerra, S., Marchetti, P., and Cardarelli, F. (2022). Single-cell imaging of α and β cell metabolic response to glucose in living human Langerhans islets. Commun. Biol. **5**:1232.

Bader, S.B., Dewhirst, M.W., and Hammond, E.M. (2020). Cyclic Hypoxia: An Update on Its Characteristics, Methods to Measure It and Biological Implications in Cancer. Cancers **13**:23.

Baena-González, E., Rolland, F., Thevelein, J.M., and Sheen, J. (2007). A central integrator of transcription networks in plant stress and energy signalling. Nature **448**:938–942.

Bailey-Serres, J., and Voesenek, L.A.C.J. (2008). Flooding Stress: Acclimations and Genetic Diversity. Annu. Rev. Plant Biol. **59**:313–339.

Barreto, P., Dambire, C., Sharma, G., Vicente, J., Osborne, R., Yassitepe, J., Gibbs, D.J., Maia, I.G., Holdsworth, M.J., and Arruda, P. (2022). Mitochondrial retrograde signaling through UCP1-mediated inhibition of the plant oxygen-sensing pathway. Curr. Biol. **32**:1403–1411.e4.

Blacker, T.S., Mann, Z.F., Gale, J.E., Ziegler, M., Bain, A.J., Szabadkai, G., and Duchen, M.R. (2014). Separating NADH and NADPH fluorescence in live cells and tissues using FLIM. Nat. Commun. **5**:3936.

Cho, H.Y., Loreti, E., Shih, M.C., and Perata, P. (2021). Energy and sugar signaling during hypoxia. New Phytol. **229**:57–63.

Contento, A.L., Kim, S.-J., and Bassham, D.C. (2004). Transcriptome Profiling of the Response of Arabidopsis Suspension Culture Cells to Suc Starvation. Plant Physiol. **135**:2330–2347.

Dalchau, N., Baek, S.J., Briggs, H.M., Robertson, F.C., Dodd, A.N., Gardner, M.J., Stancombe, M.A., Haydon, M.J., Stan, G.-B., Gonçalves, J.M., and Webb, A.A.R. (2011). The circadian oscillator gene *GIGANTEA* mediates a long-term response of the *Arabidopsis thaliana* circadian clock to sucrose. Proc. Natl. Acad. Sci. USA **108**:5104–5109.

De Clercq, I., Vermeirssen, V., Van Aken, O., Vandepoele, K., Murcha, M.W., Law, S.R., Inzé, A., Ng, S., Ivanova, A., Rombaut, D., et al. (2013). The Membrane-Bound NAC Transcription Factor ANAC013 Functions in Mitochondrial Retrograde Regulation of the Oxidative Stress Response in *Arabidopsis*. Plant Cell **25**:3472–3490.

Eysholdt-Derzsó, E., Renziehausen, T., Frings, S., Frohn, S., Von Bongartz, K., Igisch, C.P., Mann, J., Häger, L., Macholl, J., Leisse, D., et al. (2023). Endoplasmic reticulum–bound ANAC013 factor is cleaved by RHOMBOID-LIKE 2 during the initial response to hypoxia in *Arabidopsis thaliana*. Proc. Natl. Acad. Sci. USA **120**, e2221308120.

Ferri, G., Tesi, M., Massarelli, F., Marselli, L., Marchetti, P., and Cardarelli, F. (2020). Metabolic response of Insulinoma 1E cells to glucose stimulation studied by fluorescence lifetime imaging. FASEB Bioadv. **2**:409–418.

Gasch, P., Fundinger, M., Müller, J.T., Lee, T., Bailey-Serres, J., and Mustroph, A. (2016). Redundant ERF-VII Transcription Factors Bind to an Evolutionarily Conserved *cis* -Motif to Regulate Hypoxia-Responsive Gene Expression in Arabidopsis. Plant Cell **28**:160–180.

Gibbs, D.J., Lee, S.C., Isa, N.M., Gramuglia, S., Fukao, T., Bassel, G.W., Correia, C.S., Corbineau, F., Theodoulou, F.L., Bailey-Serres, J., and Holdsworth, M.J. (2011). Homeostatic response to hypoxia is regulated by the N-end rule pathway in plants. Nature **479**:415–418.

Gibbs, D.J., Md Isa, N., Movahedi, M., Lozano-Juste, J., Mendiondo, G.M., Berckhan, S., Marín-de la Rosa, N., Vicente Conde, J., Sousa Correia, C., Pearce, S.P., et al. (2014). Nitric Oxide Sensing in Plants Is Mediated by Proteolytic Control of Group VII ERF Transcription Factors. Mol. Cell **53**:369–379.

Gibbs, D.J., Tedds, H.M., Labandera, A.-M., Bailey, M., White, M.D., Hartman, S., Sprigg, C., Mogg, S.L., Osborne, R., Dambire, C., et al. (2018). Oxygen-dependent proteolysis regulates the stability of angiosperm polycomb repressive complex 2 subunit VERNALIZATION 2. Nat. Commun. **9**:5438.

Giuntoli, B., Shukla, V., Maggiorelli, F., Giorgi, F.M., Lombardi, L., Perata, P., and Licausi, F. (2017). Age-dependent regulation of ERF-VII transcription factor activity in *Arabidopsis thaliana*. Plant Cell Environ. **40**:2333–2346.

Gonzalez, N., Vanhaeren, H., and Inzé, D. (2012). Leaf size control: complex coordination of cell division and expansion. Trends Plant Sci. **17**:332–340.

Harmer, S.L., Hogenesch, J.B., Straume, M., Chang, H.-S., Han, B., Zhu, T., Wang, X., Kreps, J.A., and Kay, S.A. (2000). Orchestrated Transcription of Key Pathways in *Arabidopsis* by the Circadian Clock. Science **290**:2110–2113.

Hartman, S., Liu, Z., Van Veen, H., Vicente, J., Reinen, E., Martopawiro, S., Zhang, H., Van Dongen, N., Bosman, F., Bassel, G.W., et al. (2019). Ethylene-mediated nitric oxide depletion pre-adapts plants to hypoxia stress. Nat. Commun. **10**:4020.

Herzog, M., Pellegrini, E., and Pedersen, O. (2023). A meta-analysis of plant tissue O2 dynamics. Funct. Plant Biol. **50**:519–531. https://doi.org/10.1071/FP22294.

Holdsworth, M.J., and Gibbs, D.J. (2020). Comparative Biology of Oxygen Sensing in Plants and Animals. Curr. Biol. **30**:1979–1980.

Holdsworth, M.J., Vicente, J., Sharma, G., Abbas, M., and Zubrycka, A. (2020). The plant N-degron pathways of ubiquitin-mediated proteolysis. J. Integr. Plant Biol. **62**:70–89.

Jefferson, R.A., Kavanagh, T.A., and Bevan, M.W. (1987). GUS fusions: beta-glucuronidase as a sensitive and versatile gene fusion marker in higher plants. EMBO J. **6**:3901–3907.

Kalbácová, M., Vrbacký, M., Drahota, Z., and Melková, Z. (2003). Comparison of the effect of mitochondrial inhibitors on mitochondrial membrane potential in two different cell lines using flow cytometry and spectrofluorometry. Cytometry A. **52**:110–116.

Kim, S.W., Kim, I.K., and Lee, S.H. (2020). Role of hyperoxic treatment in cancer. Exp. Biol. Med. **245**:851–860.

Kosmacz, M., Parlanti, S., Schwarzländer, M., Kragler, F., Licausi, F., and Van Dongen, J.T. (2015). The stability and nuclear localization of the transcription factor RAP2.12 are dynamically regulated by oxygen concentration: RAP2.12 regulation by oxygen. Plant Cell Environ. **38**:1094–1103.

Kunkowska, A.B., Fontana, F., Betti, F., Soeur, R., Beckers, G.J.M., Meyer, C., De Jaeger, G., Weits, D.A., Loreti, E., and Perata, P. (2023). Target of rapamycin signaling couples energy to oxygen sensing to modulate hypoxic gene expression in *Arabidopsis*. Proc. Natl. Acad. Sci. USA **120**, e2212474120.

Labandera, A.M., Tedds, H.M., Bailey, M., Sprigg, C., Etherington, R.D., Akintewe, O., Kalleechurn, G., Holdsworth, M.J., and Gibbs, D.J. (2021). The PRT6 N-degron pathway restricts VERNALIZATION 2 to endogenous hypoxic niches to modulate plant development. New Phytol. **229**:126–139.

Lasanthi-Kudahettige, R., Magneschi, L., Loreti, E., Gonzali, S., Licausi, F., Novi, G., Beretta, O., Vitulli, F., Alpi, A., and Perata, P. (2007). Transcript Profiling of the Anoxic Rice Coleoptile. Plant Physiol. **144**:218–231.

Licausi, F., Weits, D.A., Pant, B.D., Scheible, W.-R., Geigenberger, P., and van Dongen, J.T. (2011a). Hypoxia responsive gene expression is mediated by various subsets of transcription factors and miRNAs that are determined by the actual oxygen availability. New Phytol. **190**:442–456.

Licausi, F., Kosmacz, M., Weits, D.A., Giuntoli, B., Giorgi, F.M., Voesenek, L.A.C.J., Perata, P., and van Dongen, J.T. (2011b). Oxygen sensing in plants is mediated by an N-end rule pathway for protein destabilization. Nature **479**:419–422.

Licausi, F., Giuntoli, B., and Perata, P. (2020). Similar and Yet Different: Oxygen Sensing in Animals and Plants. Trends Plant Sci. **25**:6–9.

Liu, Z., Ishikawa, K., Sanada, E., Semba, K., Li, J., Li, X., Osada, H., and Watanabe, N. (2023). Identification of antimycin A as a c-Myc degradation accelerator via high-throughput screening. J. Biol. Chem. **299**, 105083.

Loreti, E., and Perata, P. (2020). The Many Facets of Hypoxia in Plants. Plants **9**:745.

Loreti, E., Poggi, A., Novi, G., Alpi, A., and Perata, P. (2005). A genome-wide analysis of the effects of sucrose on gene expression in arabidopsis seedlings under anoxia. Plant Physiol. **137**:1130–1138.

Loreti, E., Van Veen, H., and Perata, P. (2016). Plant responses to flooding stress. Curr. Opin. Plant Biol. **33**:64–71.

Loreti, E., Valeri, M.C., Novi, G., and Perata, P. (2018). Gene Regulation and Survival under Hypoxia Requires Starch Availability and Metabolism. Plant Physiol. **176**:1286–1298.

Loreti, E., Betti, F., Ladera-Carmona, M.J., Fontana, F., Novi, G., Valeri, M.C., and Perata, P. (2020). ARGONAUTE1 and ARGONAUTE4 Regulate Gene Expression and Hypoxia Tolerance. Plant Physiol. **182**:287–300.

Lozano-Juste, J., and León, J. (2010). Enhanced Abscisic Acid-Mediated Responses in *nia1nia2noa1-2* Triple Mutant Impaired in NIA/NR- and AtNOA1-Dependent Nitric Oxide Biosynthesis in Arabidopsis. Plant Physiol. **152**:891–903.

Matsumoto, F., Obayashi, T., Sasaki-Sekimoto, Y., Ohta, H., Takamiya, K.i., and Masuda, T. (2004). Gene Expression Profiling of the Tetrapyrrole Metabolic Pathway in Arabidopsis with a Mini-Array System. Plant Physiol. **135**:2379–2391.

Michiels, C., Tellier, C., and Feron, O. (2016). Cycling hypoxia: A key feature of the tumor microenvironment. Biochim. Biophys. Acta **1866**:76–86.

Millar, A.H., Whelan, J., Soole, K.L., and Day, D.A. (2011). Organization and Regulation of Mitochondrial Respiration in Plants. Annu. Rev. Plant Biol. **62**:79–104.

Mizoguchi, T., Wheatley, K., Hanzawa, Y., Wright, L., Mizoguchi, M., Song, H.-R., Carré, I.A., and Coupland, G. (2002). LHY and CCA1 Are Partially Redundant Genes Required to Maintain Circadian Rhythms in Arabidopsis. Dev. Cell **2**:629–641.

Mockler, T.C., Michael, T.P., Priest, H.D., Shen, R., Sullivan, C.M., Givan, S.A., McEntee, C., Kay, S.A., and Chory, J. (2007). The Diurnal Project: Diurnal and Circadian Expression Profiling, Model-based Pattern Matching, and Promoter Analysis. Cold Spring Harbor Symp. Quant. Biol. **72**:353–363.

Mustroph, A., Zanetti, M.E., Jang, C.J.H., Holtan, H.E., Repetti, P.P., Galbraith, D.W., Girke, T., and Bailey-Serres, J. (2009). Profiling translatomes of discrete cell populations resolves altered cellular priorities during hypoxia in *Arabidopsis*. Proc. Natl. Acad. Sci. USA **106**:18843–18848.

Mustroph, A., Lee, S.C., Oosumi, T., Zanetti, M.E., Yang, H., Ma, K., Yaghoubi-Masihi, A., Fukao, T., and Bailey-Serres, J. (2010). Cross-Kingdom Comparison of Transcriptomic Adjustments to Low-Oxygen Stress Highlights Conserved and Plant-Specific Responses. Plant Physiol. **152**:1484–1500.

Narsai, R., Law, S.R., Carrie, C., Xu, L., and Whelan, J. (2011). In-Depth Temporal Transcriptome Profiling Reveals a Crucial Developmental Switch with Roles for RNA Processing and Organelle Metabolism That Are Essential for Germination in Arabidopsis. Plant Physiol. **157**:1342–1362.

Paul, M.V., Iyer, S., Amerhauser, C., Lehmann, M., van Dongen, J.T., and Geigenberger, P. (2016). Oxygen Sensing via the Ethylene Response Transcription Factor RAP2.12 Affects Plant Metabolism and Performance under Both Normoxia and Hypoxia. Plant Physiol. **172**:141–153.

Perata, P., and Alpi, A. (1993). Plant responses to anaerobiosis. Plant Sci. **93**:1–17.

Perata, P., Matsukura, C., Vernieri, P., and Yamaguchi, J. (1997). Sugar Repression of a Gibberellin-Dependent Signaling Pathway in Barley Embryos. Plant Cell **1**:2197–2208. https://doi.org/10.1105/tpc.9.12.2197.

Pilgrim, M.L., Caspar, T., Quail, P.H., and McClung, C.R. (1993). Circadian and light-regulated expression of nitrate reductase in Arabidopsis. Plant Mol. Biol. **23**:349–364.

Ramos-Sánchez, J.M., Triozzi, P.M., Moreno-Cortés, A., Conde, D., Perales, M., and Allona, I. (2017). Real-time monitoring of PtaHMGB activity in poplar transactivation assays. Plant Methods **13**:50.

Shukla, V., Lombardi, L., Iacopino, S., Pencik, A., Novak, O., Perata, P., Giuntoli, B., and Licausi, F. (2019). Endogenous Hypoxia in Lateral Root Primordia Controls Root Architecture by Antagonizing Auxin Signaling in Arabidopsis. Mol. Plant **12**:538–551.

Smith, A.M., and Zeeman, S.C. (2020). Starch: A Flexible, Adaptable Carbon Store Coupled to Plant Growth. Annu. Rev. Plant Biol. **71**:217–245.

Streatfield, S.J., Weber, A., Kinsman, E.A., Häusler, R.E., Li, J., Post-Beittenmiller, D., Kaiser, W.M., Pyke, K.A., Flügge, U.I., and Chory, J. (1999). The Phosphoenolpyruvate/Phosphate Translocator Is Required for Phenolic Metabolism, Palisade Cell Development, and Plastid-Dependent Nuclear Gene Expression. Plant Cell **11**:1609–1622.

Taylor-Kearney, L.J., and Flashman, E. (2022). Targeting plant cysteine oxidase activity for improved submergence tolerance. Plant J. **109**:779–788.

Tian, Y.N., Zhong, R.H., Wei, J.B., Luo, H.H., Eyal, Y., Jin, H.L., Wu, L.J., Liang, K.Y., Li, Y.M., Chen, S.Z., et al. (2021). Arabidopsis CHLOROPHYLLASE 1 protects young leaves from long-term photodamage by facilitating FtsH-mediated D1 degradation in photosystem II repair. Mol. Plant **14**:1149–1167.

Tsai, K.J., Suen, D.F., and Shih, M.C. (2023). Hypoxia response protein HRM1 modulates the activity of mitochondrial electron transport chain in Arabidopsis under hypoxic stress. New Phytol. **239**:1315–1331. https://doi.org/10.1111/nph.19006.

Van Dongen, J.T., and Licausi, F. (2015). Oxygen Sensing and Signaling. Annu. Rev. Plant Biol. **66**:345–367.

Van Dongen, J.T., Fröhlich, A., Ramírez-Aguilar, S.J., Schauer, N., Fernie, A.R., Erban, A., Kopka, J., Clark, J., Langer, A., and Geigenberger, P. (2009). Transcript and metabolite profiling of the adaptive response to mild decreases in oxygen concentration in the roots of arabidopsis plants. Ann. Bot. **103**:269–280.

Ventura, I., Brunello, L., Iacopino, S., Valeri, M.C., Novi, G., Dornbusch, T., Perata, P., and Loreti, E. (2020). Arabidopsis phenotyping reveals the importance of alcohol dehydrogenase and pyruvate decarboxylase for aerobic plant growth. Sci. Rep. **10**, 16669.

Wagner, S., Van Aken, O., Elsässer, M., and Schwarzländer, M. (2018). Mitochondrial Energy Signaling and Its Role in the Low-Oxygen Stress Response of Plants. Plant Physiol. **176**:1156–1170.

Wang, G.L., Jiang, B.H., Rue, E.A., and Semenza, G.L. (1995). Hypoxia-inducible factor 1 is a basic-helix-loop-helix-PAS heterodimer regulated by cellular O2 tension. Proc. Natl. Acad. Sci. USA **92**:5510–5514.

Webb, A.A.R. (2003). The physiology of circadian rhythms in plants. New Phytol. **160**:281–303.

Weits, D.A., Giuntoli, B., Kosmacz, M., Parlanti, S., Hubberten, H.-M., Riegler, H., Hoefgen, R., Perata, P., van Dongen, J.T., and Licausi, F. (2014). Plant cysteine oxidases control the oxygen-dependent branch of the N-end-rule pathway. Nat. Commun. **5**:3425.

Weits, D.A., Kunkowska, A.B., Kamps, N.C.W., Portz, K.M.S., Packbier, N.K., Nemec Venza, Z., Gaillochet, C., Lohmann, J.U., Pedersen, O., van Dongen, J.T., and Licausi, F. (2019). An apical hypoxic niche sets the pace of shoot meristem activity. Nature **569**:714–717.

Weits, D.A., van Dongen, J.T., and Licausi, F. (2021). Molecular oxygen as a signaling component in plant development. New Phytol. **229**:24–35.

White, M.D., Klecker, M., Hopkinson, R.J., Weits, D.A., Mueller, C., Naumann, C., O'Neill, R., Wickens, J., Yang, J., Brooks-Bartlett, J.C., et al. (2017). Plant cysteine oxidases are dioxygenases that directly enable arginyl transferase-catalysed arginylation of N-end rule targets. Nat. Commun. **8**, 14690.

Zubrycka, A., Dambire, C., Dalle Carbonare, L., Sharma, G., Boeckx, T., Swarup, K., Sturrock, C.J., Atkinson, B.S., Swarup, R., Corbineau, F., et al. (2023). ERFVII action and modulation through oxygen-sensing in Arabidopsis thaliana. Nat. Commun. **14**:4665.